AeroTactic Company

presents the

FF-1 Rainbird

In response to the 2015-2016 AIAA Foundation Graduate Team Aircraft Design Competition

Presented by California State Polytechnic University, Pomona

Aerospace Engineering Department

Aircraft Design 2015-2016

CAL POLY POMONA

AeroTactic Company Team

Program Manager
Stephanie Chavez

Aerodynamics
Sean Hui

Chief Systems Engineer,
Geraldson Evangelista

Economics
Gabriel Buenrostro

Stability and Control
Raghav Handa

Configurations
Garun Arustamov

Structures
David Hunter

Propulsion
Camila Franco

Performance and Mission Design
Cynthia Garcia

Interior Design, Quick Loading
Bill Wogahn
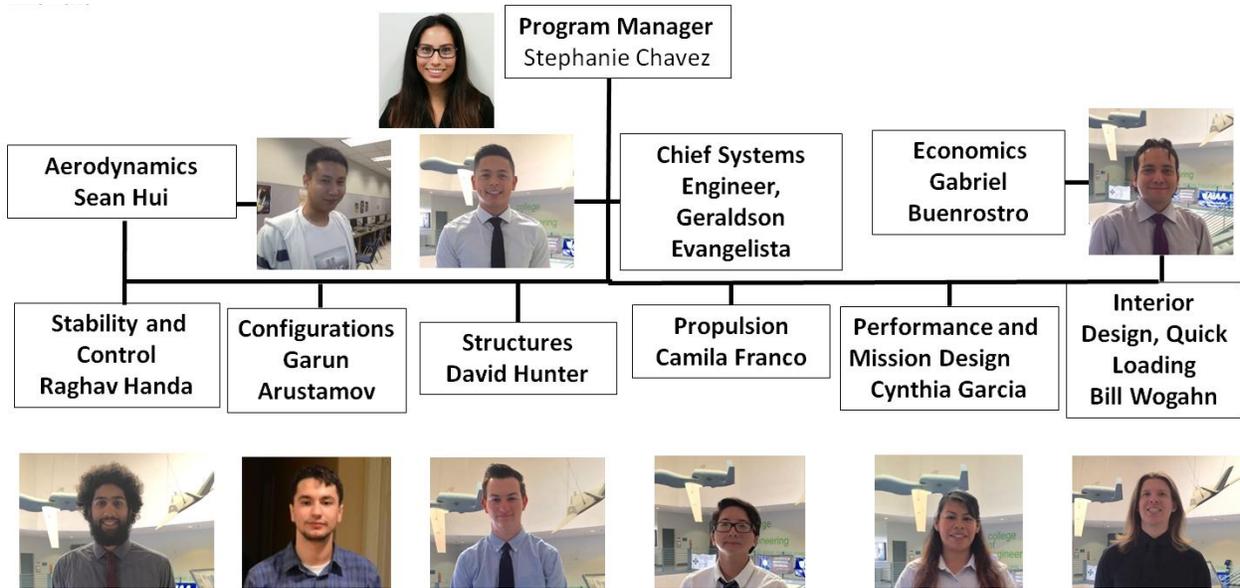
Team AIAA Member Numbers

Arustamov, Garun	Configurations	688375	garustamov@cpp.edu
Buenrostro, Gabriel	Economics	688306	buen63@aol.com
Chavez, Stephanie	Program Manager	688201	smulloa21@gmail.com
Evangelista, Geraldson	Chief Systems Engineer	516760	geraldsonbe@gmail.com
Franco, Camila	Propulsion	688628	acfranco@cpp.edu
Garcia, Cynthia	Performance/Mission Design	688308	g.cynthia1225@yahoo.com
Handa, Raghav	Stability and Control	688330	rhanda007@yahoo.com
Hui, Sean	Aerodynamics	688578	seanhui55555@hotmail.com
Hunter, David	Structures	688304	dbh2024@gmail.com
Wogahn, Bill	Interior Design/ Quick Loading	688621	wogahnb@yahoo.com
Dr. Don Edberg	Project Advisor	022972-00	dedberg@cpp.edu

Executive Summary

The AeroTactic Company would like to present the FF-1 Rainbird in response to the 2015-2016 American Institute of Aeronautics and Astronautics (AIAA) Graduate Team Aircraft Design Competition Request for Proposal (RFP). The RFP was received by the AeroTactic Company on September 24, 2015. It expressed the desire for the design of a "purpose-built large size firefighting aircraft" that possesses an Entry Into Service (EIS) date of 2022 and a design lifetime of 20 years or greater. The RFP specified that the aircraft shall carry a payload of 5,000 gallons (retardant or water) with an operational radius of 200 nm. The aircraft shall also meet a ferry range of 2,500 nm. In addition, it shall possess a balanced field length of 5,000 ft and be able to takeoff from 5,000 ft above mean sea-level with +35°F standard atmosphere. The aircraft shall drop at an altitude below 300 ft at a speed below 150 kt, while still having a stall speed of 90 kt. On the return trip from the fire mission, the aircraft shall have a dash speed greater than 300 kt. The retardant reload time shall not exceed 10 min with engines on and the aircraft shall possess a turbine engine with an off-the-shelf engine being preferred. The aircraft shall also meet FAA certification for a transport aircraft (Part 25) with special attention to fatigue. According to the RFP, the aircraft should also minimize the time needed to establish a fireline as well as the cost of ownership. The FF-1 Rainbird aircraft design, submitted by the AeroTactic Company, features an integrated payload tank capable of carrying a 5,000 gallons (47% greater than the C-130's maximum payload) of retardant/water with a gravity fed dispersal system. It also possesses two Rolls Royce Tay turbofan engines underneath the wings. Winglets increased the Rainbird's L/D by 5%, consequently increasing its fuel efficiency (all fuel necessary is located within the wings). The Rainbird's integrated payload tank is capable of being reloaded within five and a half minutes. It reloads 43 times faster than the C-130's pressurized MAFFS II system and two and a half minutes faster than the DC-10's gravity system's fastest time of eight minutes (typical reload is 15-20 min). With a unit price of $49.8M (in 2022 $), the FF-1 Rainbird costs 28.5% less than retrofitting a C-130 ($69.6M in 2022 $) and 11.1% less than the DC-10 ($56M in 2022 $). In addition, the Rainbird costs 4.6% less than purchasing an already retrofitted C-130, $52.2 in 2022 $ (including depreciation of the C-130).

57.95 111.35

64.80

3

Table of Contents

List of Figures

List of Tables

List of Acronyms

AIAA = American Institute of Aeronautics and Astronautics

AOA = Angle of Attack

AR = Aspect Ratio

CG = Center of Gravity

DOC = Direct Operating Cost

EIS = Entry Into Service

FAA = Federal Aviation Administration

FLIR = Forward Looking Infrared

FRDS = Fire Retardant Dispersal System

GSE = Ground Support Equipment

LOX= Liquid Oxygen

MAC = Mean Aerodynamic Center

MAFFS = Modular Airborne Fire Fighting Systems

MTOW = Maximum Takeoff Weight

N.A.C.A. = National Advisory Committee for Aeronautics

OEI = One Engine Inoperative

RDT&E= Research, Develop, Test, and Evaluation

RFP = Request for Proposal

SFC = Specific Fuel Consumption

List of Symbols

AR = Aspect Ratio

C = Chord

C_D = Coefficient of Dragon

C_{Di} = Induced Drag

C_{Dp} = Parasite Drag

C_L = Coefficient of Lift

e = Efficiency

l_h = Distance From CG to 25% MAC Horizontal Tail

L/D= Lift to Drag

S = Area of wing (ft^2)

S_h = Horizontal Tail Area

S.M. = Static Margin

T/W = Thrust to Weight Ratio

V = Speed (knots)

V_h = Horizontal Volume Coefficient

W = Weight (lb)

W/S = Wing Loading (lb-f/ft^2)

X$_{np}$ = Neutral Point Location from the Nose of Aircraft (ft)

X$_{cg}$ = Center of Gravity Location from the Nose of Aircraft (ft)

δ = Deflection Angle of Flaps (Degrees)

ρ = Density (μ/ft^3)

μ = Slugs

1. Requirements Overview

According to the RFP, the aircraft shall be designed to carry a payload of 5,000 gallons (retardant or water) with an operational radius of 200 nm and three retardant drops per sortie. The aircraft shall also meet a ferry range of 2,500 nm. In addition, it shall possess a balanced field length of 5,000 ft and be able to takeoff from 5,000 ft above mean sea-level with +35°F standard atmosphere. The aircraft shall drop at an altitude below 300 ft at a speed below 150 kt, while still having a stall speed of 90 kt. On the return trip from the fire mission, the aircraft shall have a dash speed greater than 300 kt. The retardant reload time shall not exceed 10 min with engines on and the aircraft shall possess a turbine engine with an off-the-shelf engine being preferred. If the aircraft design will require a crew, the crew shall consist of two individuals. The aircraft shall also meet FAA certification for a transport aircraft (Part 25) with special attention to fatigue. According to the RFP, the aircraft should also minimize the time needed to establish a fireline, assuming that four sorties successfully establish a fireline. The design should also be cognizant of the sensing and actuation equipment needed in order to provide a fireline. In addition, the aircraft should minimize the cost of ownership.

2. Mission Analysis

The RFP states that the aircraft design must be able to carry 5,000 gallons of either water or retardant. The aircraft design shall possess an operational radius of 200 nm and complete a turn between three equal drops. The aircraft shall also have a ferry range of 2,500 nm. Figure 2-1 shows the two mission profiles (fire mission and ferry mission) that the Rainbird was designed to perform. For the fire mission, the Rainbird will takeoff from 5,000 ft +35°F standard atmosphere (density of 0.0019 slugs/ft^3). It will then climb to 20,000 ft above mean sea-level and cruise 200 nm to the fire at a Mach number of 0.4 (245.6 kt). Once the Rainbird reaches the fire, it will

loiter to assess the fire and determine where to establish the fireline. After loitering, the Rainbird will descend to below 300 ft above the fire and complete its three equal payload drops with a full turn in between drops. It will then ascend back to cruise altitude and return to base (200 nm away) at a speed of 300.4 kt. (The fuel needed and payload range was determined with a dash speed of 300.4 kt, however, according to the operational envelope, the Rainbird is capable of dashing at a speed up to 387 kt.) Back at base, the Rainbird will loiter before descending for landing and reloading. For the ferry mission, the Rainbird will also takeoff from 5,000 ft +35°F standard atmosphere and climb to a cruise altitude of 20,000 ft. It will cruise for 2,500 nm until it reaches its destination. The Rainbird will then loiter before descending to 5,000 ft for landing.

The AeroTactic Company also considered whether or not the aircraft design benefitted most from being piloted or unpiloted. Due to the vitality of situational awareness while flying into forest fire terrain, a piloted aircraft would be more beneficial than an unmanned aircraft. A piloted aircraft is more flexible to changing scenarios compared to a UAV. In addition, an unpiloted aircraft would cost more to maintain and to build due to the additional sensors, hardware, and software required. Thus, AeroTactic decided to design the Rainbird as a piloted aircraft.
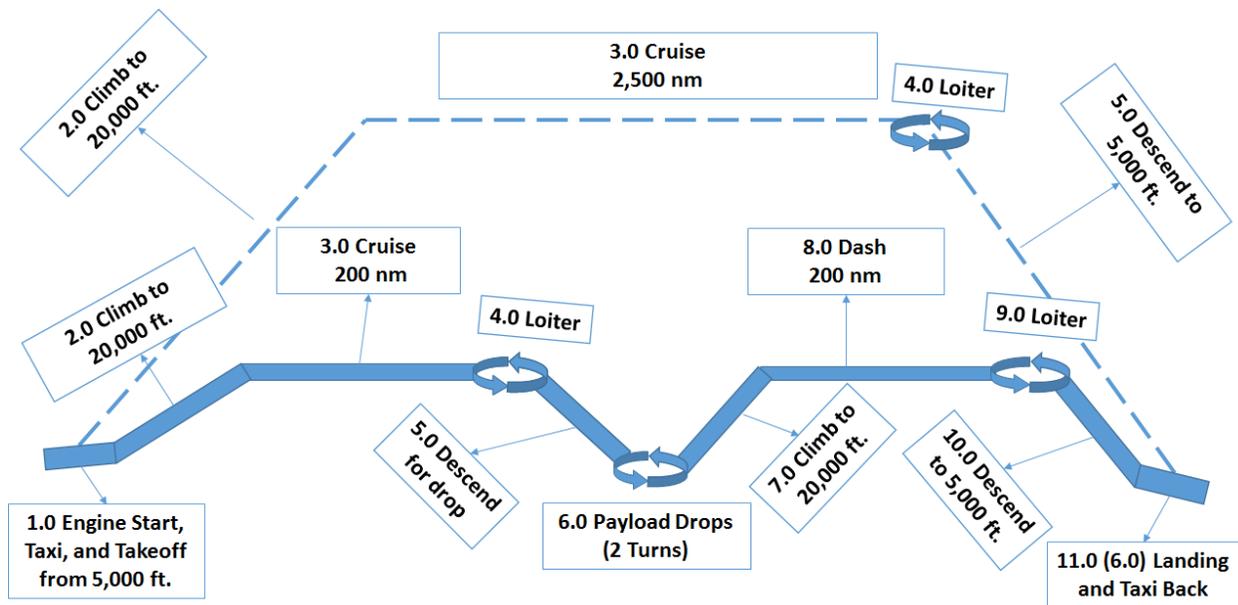
Figure 2-1 The mission profile for both missions (fire and ferry) of the FF-1 Rainbird.

3. Configuration Overview

The FF–1 Rainbird was designed and configured in order to best fulfill its payload and performance requirements. The RFP states that the aircraft shall be able to carry 45,000 pounds of fire retardant, a payload of 5,000 gallons in volume. The aircraft also must also be able to fly at speeds as low as 90 knots. The high density payload combined with the low stall speed requirement drove the design of the aircraft to contain large wings and a small fuselage. The fuselage is optimally configured to house a cabin for two pilots, carry a large payload tank, and provide a moment arm for the tails in order to properly control the aircraft. The large air tanker is powered by two Rolls Royce Tay 620 turbofan engines, which are attached to the wing's leading edge. The engines protrude past the wing in order to balance the aircraft for all loading configurations. The aircraft is designed to be compact, resilient, and mission ready as it is capable of carrying enough fuel for four sorties and is able to reload its payload within ten minutes.
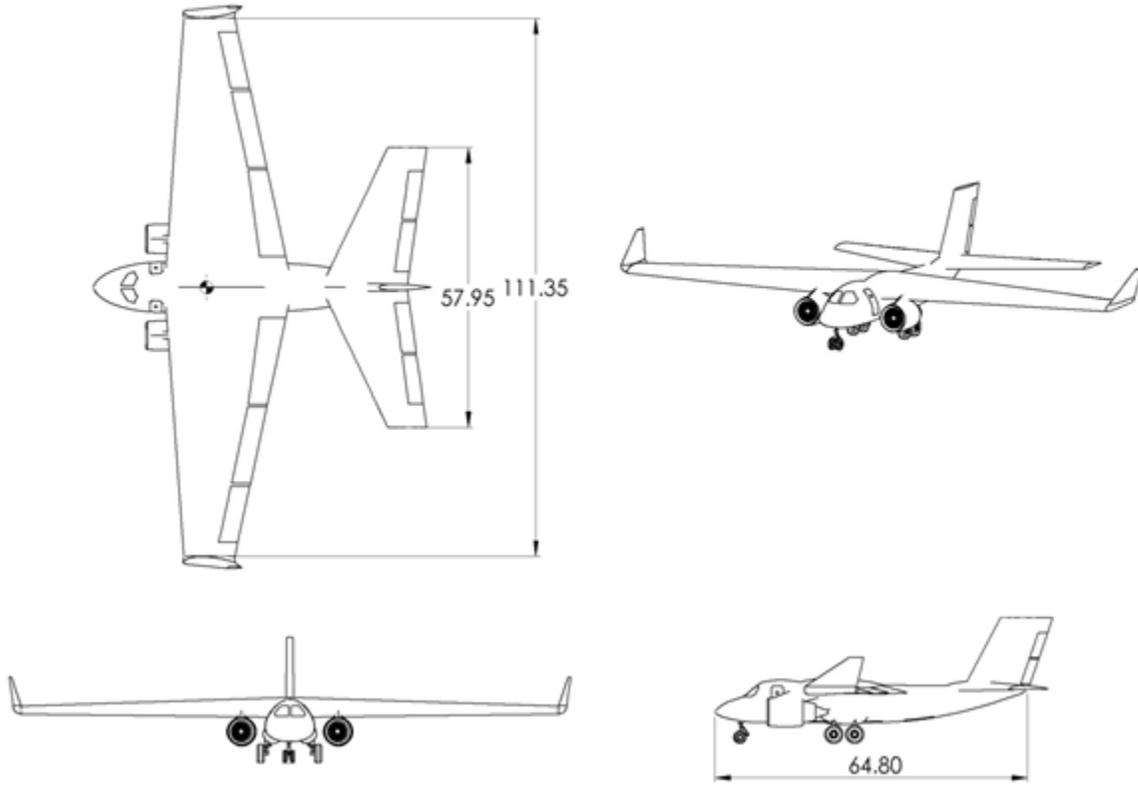
Figure 3-1: Top, front, side, and isometric view of the large air tanker FF–1 Rainbird

Table 3-1: Overview of the FF-1 Rainbird Large Air Tanker

Engine Type	Rolls Royce Tay 620
Total Thrust	27,700 lb
Maximum Payload	45,000 lb
MTOW	89,197 lb
Cruise Mach	0.45

The Rainbird features a tricycle landing gear aircraft containing oleo struts. The landing gear is deployed during takeoff and landing, and is stowed away into external pods during all other portions of flight. Fowler flaps are incorporated as the control surfaces since they provide a large increase in lift coefficient and a moderate increase in weight. The large air tanker also features winglets as a means of reducing drag, thus further condensing the overall size and reducing the maximum takeoff weight of the airplane. The winglets are tilted outward from the vertical in order to provide lift as well as reduce drag. The aerodynamics of the winglets were analyzed using Desktop Aeronautics Linair, which resulted in an increase of over 5% in lift to drag ratio. A conservative increase in the lift to drag ratio of 5% was used during sizing of the aircraft.
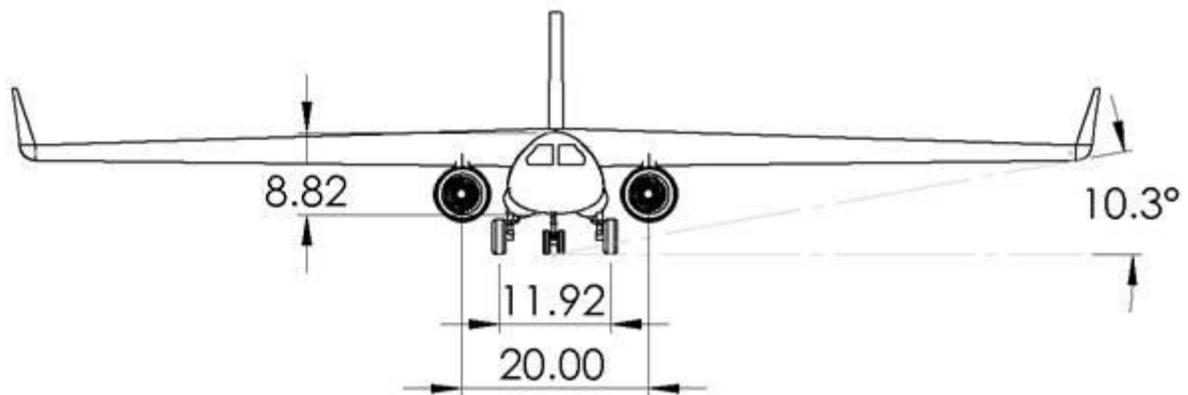
Figure 3-2: Front view of the large air tanker

The payload of the aircraft is stored within a single integrated tank. The tank is shaped as a modified oval and contains baffles that diminish sloshing effects. It can be accessed from the underside as the drop doors open for maintenance. A man-sized access door is included aft of the payload tank for maintenance of electrical equipment and general structural components.
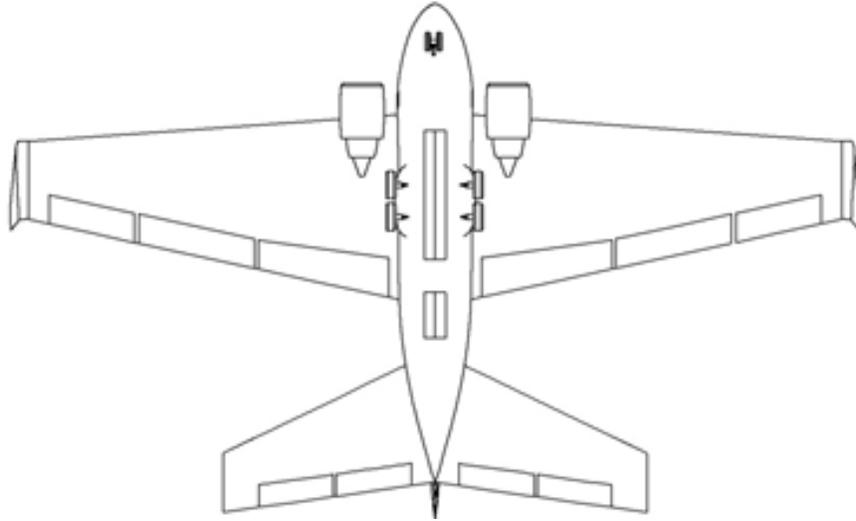
Figure 3-3: Underside of the FF-1 showing the drop doors and access doors

The aircraft features the Trotter Controls FRDS Gen II dispersal Control System, which is capable of releasing the payload through the drop doors at any time for any given duration. The payload is refilled with three hoses through either the left or the right side of the fuselage. The tanker also features a raised cabin for a broad and open view for the pilots.
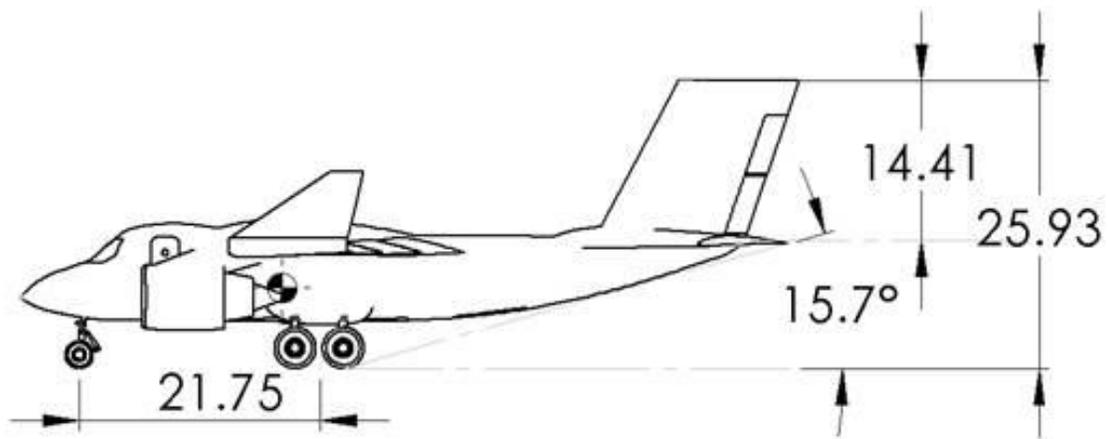
Figure 3-4: Side view of the FF–1

4. Payload Integration

The tank for the payload was decided to be an integrated design as opposed to other removable designs commonly used such as the MAFFS II. Removable designs tend to take upwards of about 30 minutes to an hour to be removed from the aircraft, refueled, and replaced. Integrated tanks are only dependent on how many hoses are available and the flow rate of each hose, thus, we have the ability to meet the required 10 minute reload time. The integrated tank used for the FF-1 design can be seen below in Figure 4-1.
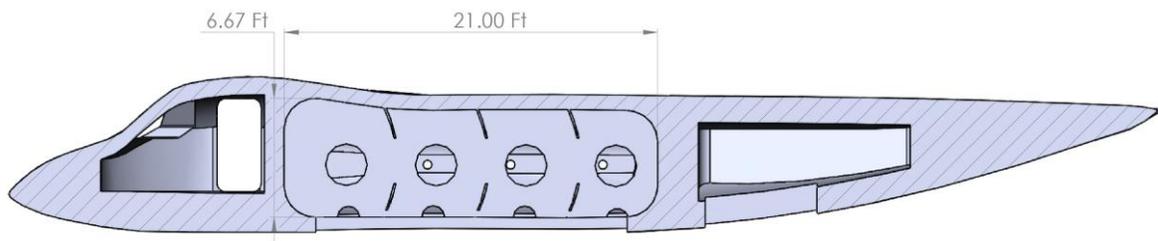
Figure 4-1 Integrated Payload Tank and Fuselage Dimensions

The integrated tank has a length of 21.78 feet, a height of 6.01 feet, and a width of 8.00 feet. These dimensions were selected in order to meet the 5,000 gallon payload requirement while keeping the center of gravity centered upon the CG of the aircraft, limiting CG shift during payload drops. It was also designed with the intention of keeping the aircraft space efficient; allowing for the fuselage to be as small as possible while still being long enough to maintain aircraft stability, hence the larger length of the tank relative to its other dimensions. Lastly, a modified oval cross-section was selected over a purely cylindrical design in order to implement the baffling system discussed below in section 4.3. Since the tank will be non-pressurized, the modified oval design will not have additional stresses commonly seen in pressurized tanks.

4.1 Payload Weight

The RFP requires that 5,000 gallons of either fire retardant or water must be carried by the large air tanker. As defined by the RFP, the fire retardant payload is assumed to have a density of 9 lb/gal, giving a total weight of 45,000 lb. The maximum density of water is 8.3 lb/gal, giving a total weight of approximately 41,500 lb. Considering this, the fire retardant was used to estimate the maximum payload weight, being that it represented the maximum possible payload weight scenario.

4.2 Baffling System

The existence of contained fluid on the aircraft creates a sloshing effect that could potentially affect aircraft dynamics. This is due to the natural frequencies of the sloshing fluid causing dynamic loads which create added forces and moments such as pitching moments, rolling moments, lateral forces, and longitudinal forces. Sloshing can also cause large shifts in the center of gravity which could affect the stability of the aircraft in flight. In order to mitigate some of the stability issues caused by sloshing, it was decided that a baffling system would be implemented. [6] From a research paper titled Effect of Tank Cross-Section and Longitudinal Baffles on Transient Liquid Slosh in Partly-Filled Road Tankers, a baffling system (shown below in figure 4.2-1) was selected.
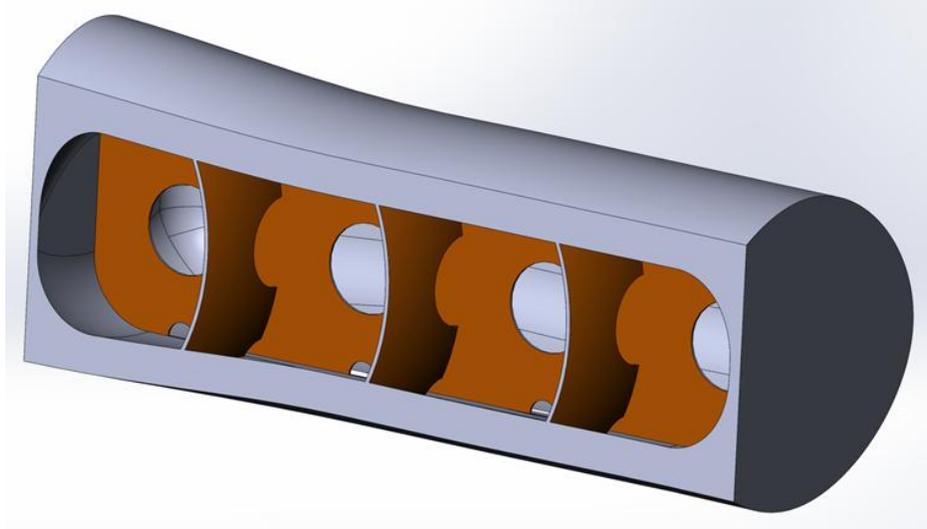
Figure 4.2-1 Baffling System for Integrated Payload Tank

The baffling system shown features one lengthwise panel with three evenly spaced cross-sectional panels, each having varying perforations to allow for some flow between the individual compartments. This setup significantly reduces the impact of the sloshing effect by limiting center of gravity travel along with the effects on rolling and pitching moments, all while adding minimal weight to the system.

4.3 Dispersal System

The main requirement for the payload drop system was that it needed to perform at least three drops per sortie. In order to accomplish this task, a third-party system was implemented. The Fire Retardant Dispersal System (FRDS) Gen II by Trotter Controls is a system currently in use by the Air Tractor 802F, a firefighting air tanker that operates with a single payload tank similar to that used in the FF-1 "Rainbird". Due to the FF-1's integrated payload tank being a single tank design, the Trotter Controls dispersal system could be implemented into the system as is, without major modifications. The advantages of using the FRDS Gen II as opposed to creating a dispersal system in house is that the FRDS can be programmed to perform any number

of drops while simultaneously controlling the individual drop volumes and drop spread, two elements that are crucial for obtaining maximum effectiveness for a single drop. These settings can also be programmed prior to the drop with the control panel (shown below in figure 4.3-1) by one of the pilots, allowing them to focus on the mission.

Figure 4.3-1 Trotter Controls FRDS Gen II Control Panel

Trotter Controls has also included an online training manual for operating their dispersal system, making it simple for any FRDS operator to access it and learn how to use the system.

4.4 Ground Support Equipment (GSE) and Reload Time

In order to meet the 10 minute reload time requirement specified in the RFP, it is important to address what equipment will be needed at each operating fire station. First, at least three hoses, each connected to a separate fire retardant/water reservoir, must be present at each fire station. (Three ports have been incorporated on each side of the FF-1.) Each hose has an

optimum flow rate of about 300 gal/min, meaning that three hoses operating at the same time can refill the total 5,000 gallons in approximately five and a half minutes, giving ground crews plenty of time to set up and remove refueling equipment. Fortunately, all fire stations in the U.S. that are geared to accommodate large air tankers have all of the necessary equipment and infrastructure needed for the FF-1 integrated tank, eliminating the need for additional ground equipment that would drive up program costs.

5. Initial Sizing

A constraint diagram was constructed for both a turboprop and turbofan design. Constraint lines on Figure 5-1 and Figure 5-2 were constructed from the RFP requirements. Four different types of high lift devices were considered for the design: split flaps, hinged flaps, zap flaps, and fowler flaps. This resulted in four possible design points within the "design space" of the constraint diagrams. With a MTOW of 89,197 lb the least amount of power and thrust required according to the four possible design points would be 13,380 hp and 13,380 lb_f according to the lowest thrust to weight ratio of the turbofan and turboprop constraint diagrams. Due to the power limitations of a turboprop, the only turboprop capable of meeting the power needed is the Europrop TP400 which weighs 25.7% more than the heaviest turbofan being considered. Thus, AeroTactic decided not to move forward with a turboprop design (further discussed in Section 6.5: Turboprop and Turbofan Comparison).
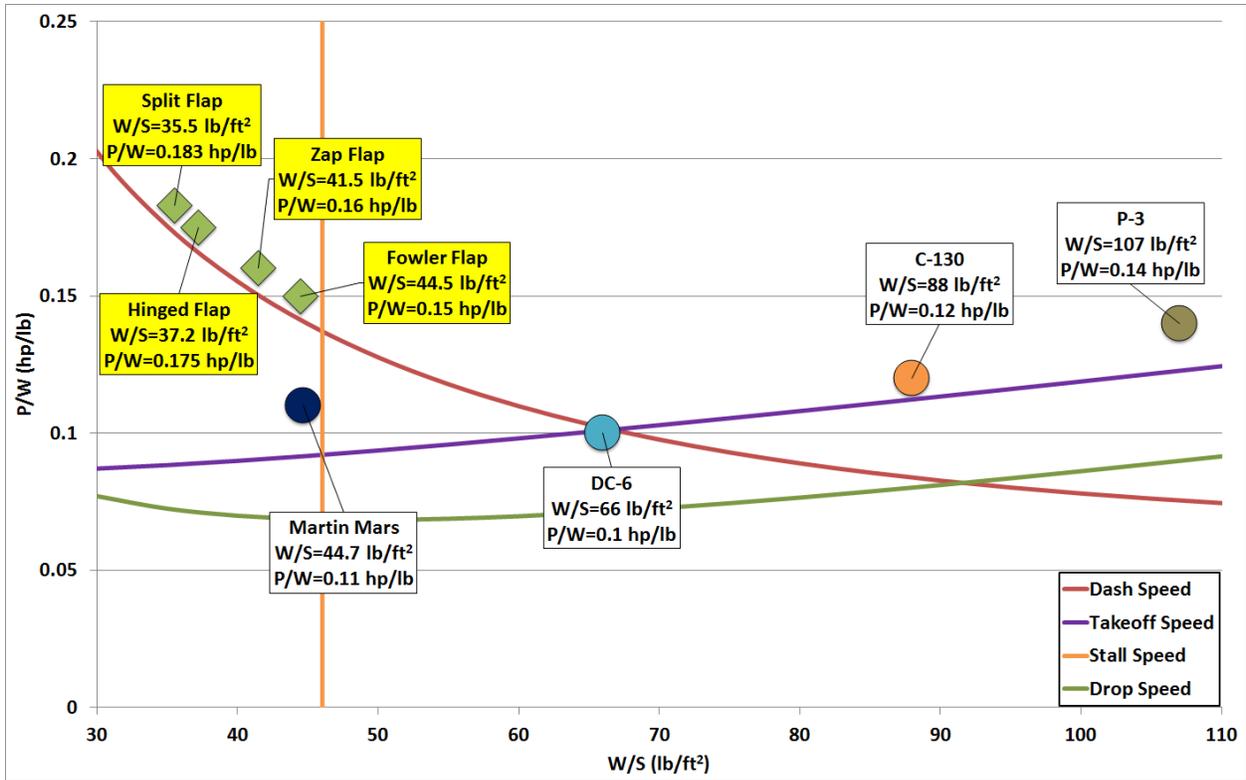
Figure 5-1 The constraint diagram used for the determination of the FF-1 turboprop wing loading and power-to-weight ratio.
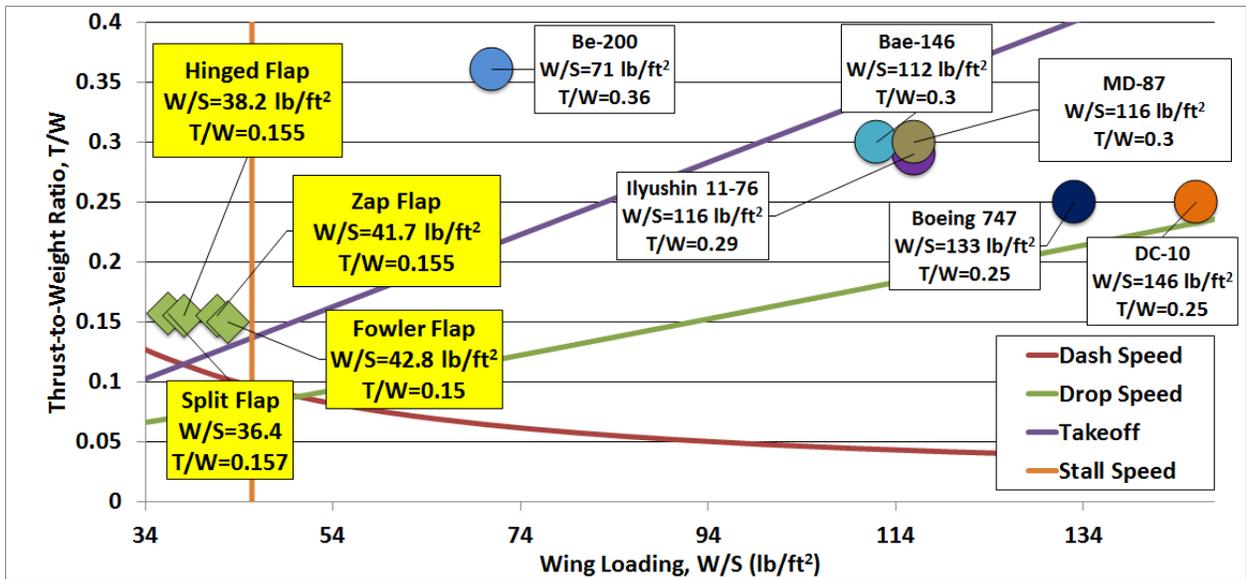
Figure 5-2 The constraint diagram used for the determination of the FF-1 turbofan wing loading and thrust-to-weight ratio.

6. Wing and Propulsion Selection

With possible design points identified, AeroTactic continued on with the wing airfoil selection, a trade study on the benefits of winglets, and a trade study encompassing of aspect ratio, lifting surface, and propulsion combinations.

6.1 Wing Airfoil Selection

An investigation was performed in order to find the most suitable airfoil for the wing of the Rainbird. The selection was made from N.A.C.A. airfoils using data from Abbott and Von Doenhoff's Theory of Wing Sections.[1] The choice was made by first researching the advantages and disadvantages of four, five, and six-digit airfoil categories. It was found that six-digit airfoils are commonly optimized for laminar flow whereas four-digit airfoils are optimized for low speed lift. Five-digit airfoils were found to have poor stall characteristics compared to four-digit airfoils that have relatively superior high angle of attack performance characteristics. Four-digit airfoils are also not easily susceptible to roughness, a feature very beneficial when flying over hazardous terrain, thus the choice was narrowed down to four-digit airfoils. Next, the highest performing airfoil was chosen by comparing maximum lift coefficient and parasitic drag values of four-digit airfoils at 9E+6 Reynolds number with no flap deflection. The N.A.C.A. 4415 was chosen because it had an approximate maximum lift coefficient of 1.6 and a parasitic drag value of approximately 0.0065. The thickness ratio of fifteen percent provides an ideal volume for storage of fuel. Accordingly, the N.A.C.A. 4415 was selected as the most optimum airfoil.
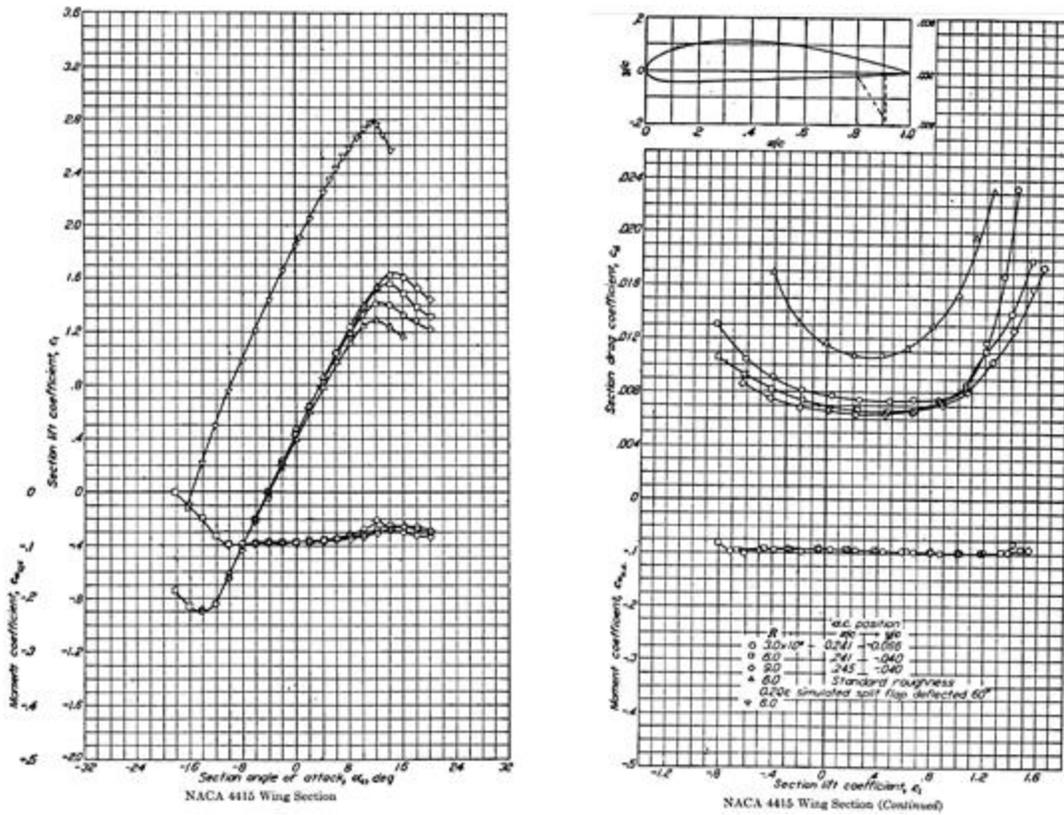
Figure 6.1-1: Wing section lift curve slope and drag polar for the N.A.C.A. 4415 Airfoil

6.2 Winglet Trade Study

The winglets added to the FF-1 design were the result of a trade study comparing L/D of the main wing with and without winglets, as shown below in Figure 6.2-1.
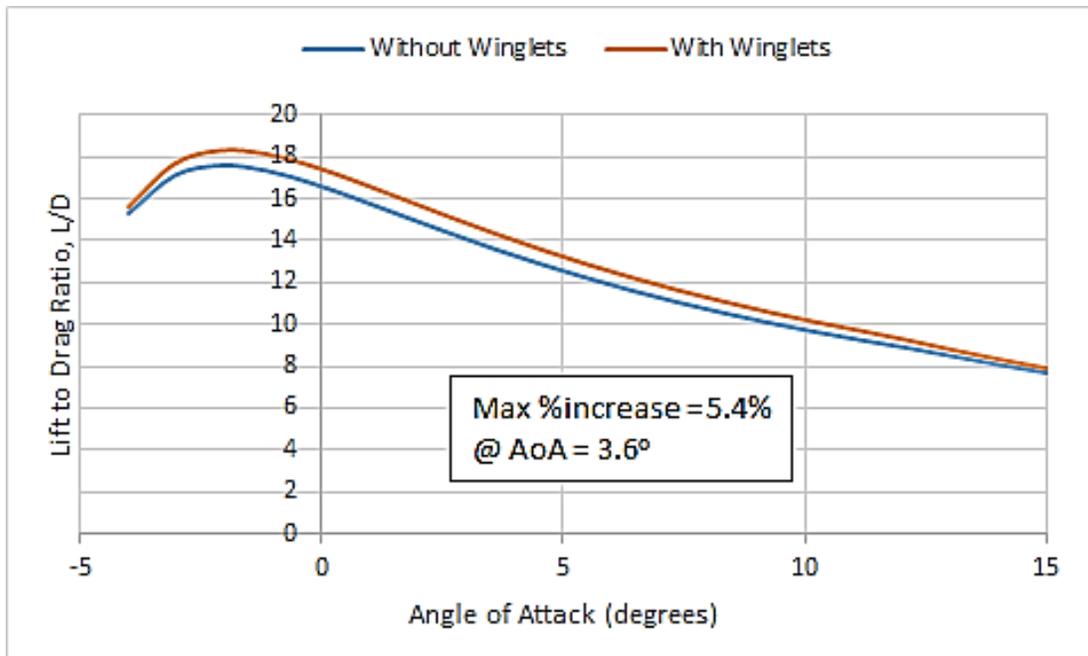
Figure 6.2-1 Lift to Drag Ratio With and Without Winglets

As shown by the figure above, There's a significant increase in the lift to drag ratio, having a maximum increase of about 5.4%. Due to this increase in L/D, it was found that the total fuel weight could be decreased by about 635 lb, or about 4.5%, while adding roughly 107 lb for the weight of the winglet. This decreases the total weight of the aircraft by 528 lb and saves over $4,600 in fuel costs per mission, providing significant savings over the lifespan of the FF-1 program. The winglets were thus included into the design, assuming a conservative five percent increase to L/D, in order to reduce the size of the overall aircraft and save on cost.

6.3 Aspect Ratio, Lifting Surface, and Propulsion Trade Study

A trade study was conducted in order to determine the optimal aspect ratio, flap, and engine combination. The aspect ratios ranged from five to 11 in increments of one. As previously mentioned, four flap types were considered for the design. Four turbofan engines were also selected: Rolls Royce Tay 620, Rolls Royce AE3007H, GE CF34-3B1, and GE CF34-8C5B1.

AeroTactic wanted to determine whether the extra weight imparted onto the aircraft from the

flaps would be compensated by the additional lift that they provide. In addition, Table 6.3-1

shows that Rolls Royce Tay 620 possesses the lowest SFC (0.45) of the four engines, yet it has

the highest combined weight (lb). AeroTactic desired to ascertain whether the Tay's lower SFC

would compensate its heavier weight.

<div align="center">Table 6.3-1 Engine Data</div>

Engine	Thrust (lb_f)	SFC (lb/lb_f-hr)	Weight (lb)	Combined Total Weight (lb)	Number of Engines Required
Rolls Royce Tay 620 [13]	13,850	0.45	3,300	6,600	2
Rolls Royce AE 3007H [13]	9,500	0.64	1,600	3,200	2
GE CF34-8C5B1 [13]	13,790	0.67	2,400	4,800	2
GE CF34-3B1 [13]	9,220	0.69	1,700	3,400	2

The carpet plots shown in Figure 6.3-1 identify that the optimal aspect ratio, flap, and

engine combination for the FF-1 Rainbird design is an aspect ratio of six, a fowler flap, and the

Rolls Royce Tay 620 shown in the green dot to the left of the plot. That combination meets all

design constraints with the lowest maximum takeoff weight (89,197 lb). The second green dot to

the right shows the backup design point. The backup design point, which utilizes the GE CF34-

8C5B1 engine, aspect ratio of 6, and a fowler flap would be the next optimal point, and is

selected in order to mitigate risks of engine procurement such as late delivery or recall.
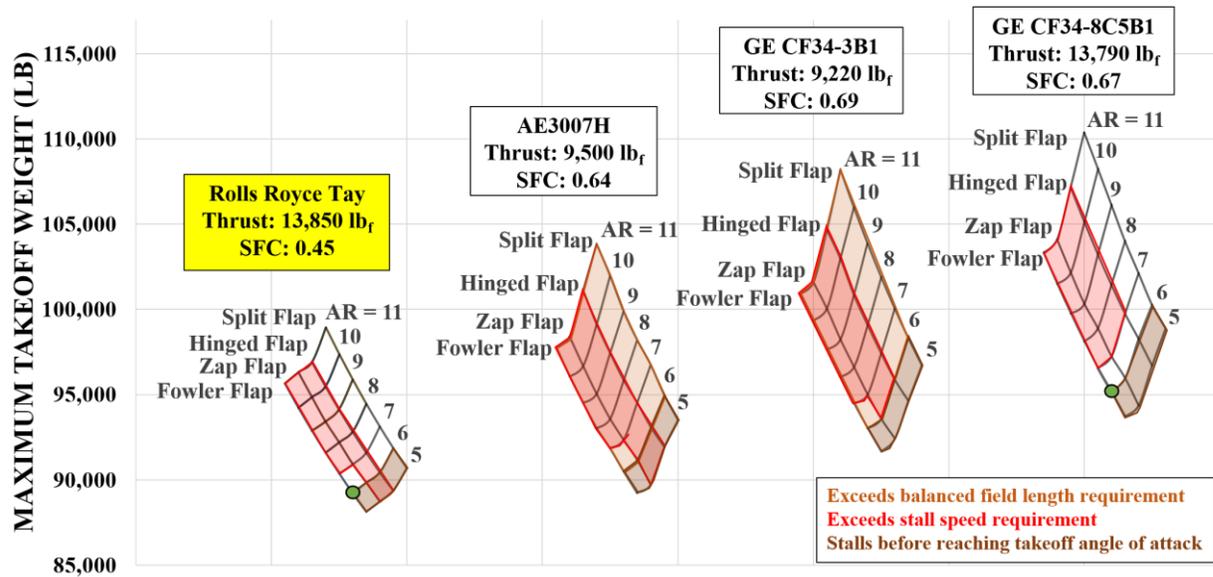
Figure 6.3-1: Effect of Aspect Ratio, Flaps, and Engines on MTOW

6.4 Selected Propulsion System and Alternate Propulsion System Financial Comparison

Although, the primary propulsion system was found to be 1.5% more in costs than the secondary propulsion system, its SFC of 0.45 lb/lb$_f$-hr compared to the SFC of 0.67 lb/lb$_f$-hr for the 8C5B1 will prove to have lower operating costs. Table 6.4-1 displays the engine and costs associated with the primary followed by the secondary engine.

Table 6.4-1 Primary and Secondary Engine and Cost Comparison

Engine	Costs (2022 $)
Rolls Royce Tay 620	8,630,000
GE CF34-8C5B1	8,490,000

6.5 Turboprop and Turbofan Comparison

The engine selection was initiated by investigating different types turboprop and turbofan engines. The engine selection had several categories; thrust/horsepower, weight, specific fuel

consumption, and whether it was currently in production. The thrust required for our design was obtained from the constraint diagram based on the restraining conditions such as takeoff altitude of 5,000 ft with +35 °F, a dash speed greater than 300 kt, and a stall speed of 90 kt. With a thrust-weight ratio of 0.15 and an aircraft takeoff weight of 89,197 lb, the thrust required is 13,379 lb_f or 12,333 hp. After investigating several engines, it was determined that turboprop engines were not ideal options. This conclusion was made after calculating that the amount of turboprop engines needed in our design ranged from two to four because turboprop engines have a horsepower range of 2,000-11,000 [10]. A turboprop engine comparison is shown in Figure 6.5-1.
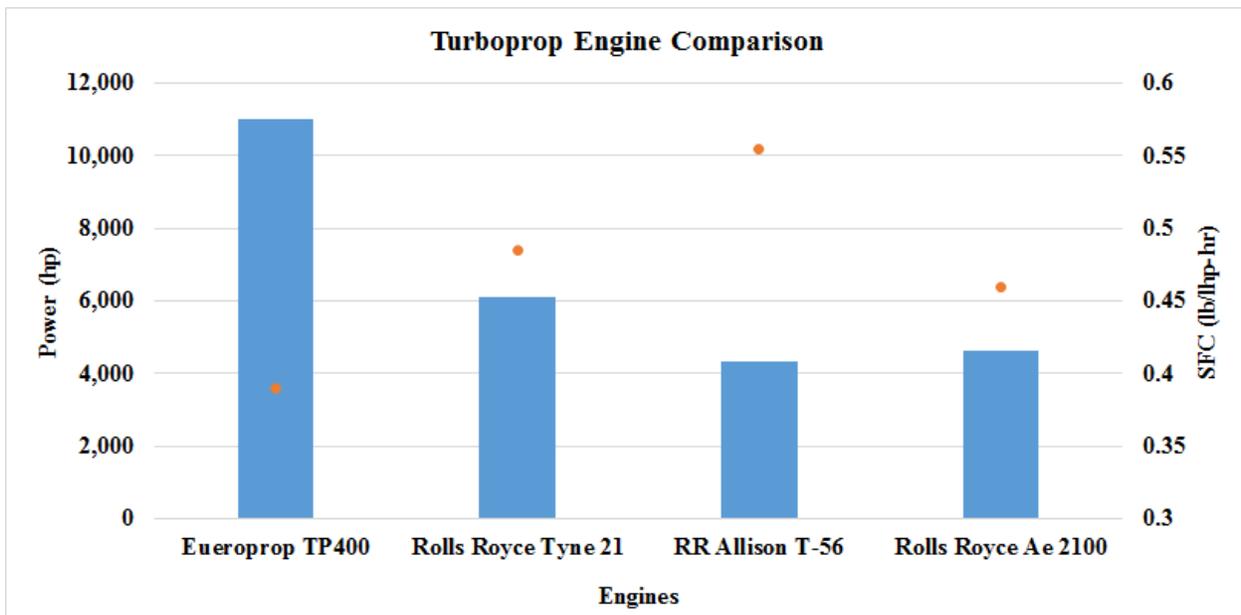
Figure 6.5-1 Turboprop Engine Thrust and SFC Comparison

The Europrop TP400 was the only engine that could provide enough thrust with only two engines. (AeroTactic determined that two engines were most beneficial for maintenance time and cost.) However, the Europrop TP400 was going to increase the total aircraft weight by 20%. In addition, there is not a backup turboprop that can provide enough horsepower with only two engines.

The design included two turbofan engines because of the benefits of a lower cost in engine maintenance and maximum aircraft weight. Turbofan engine thrust ranges from 2,000 to 20,000+ lb_f. The turbofan engines selected to conduct a series of trade studies were the General Electric CF-34 family [2], as well as the 3007H and Tay 620 engines from the Rolls Royce family [13]. Both manufacturers have engines with a thrust range of 9,000 and 13,000 lb_f and a specific fuel consumption range of 0.4 and 0.6. The turbofan engine comparison is shown in Figure 6.5-2. The engine selected for the Rainbird was Rolls Royce Tay 620 because it was the only engine that met all requirements with the lightest MTOW and the back-up engine selected was the General Electric CF34-8C5B1.
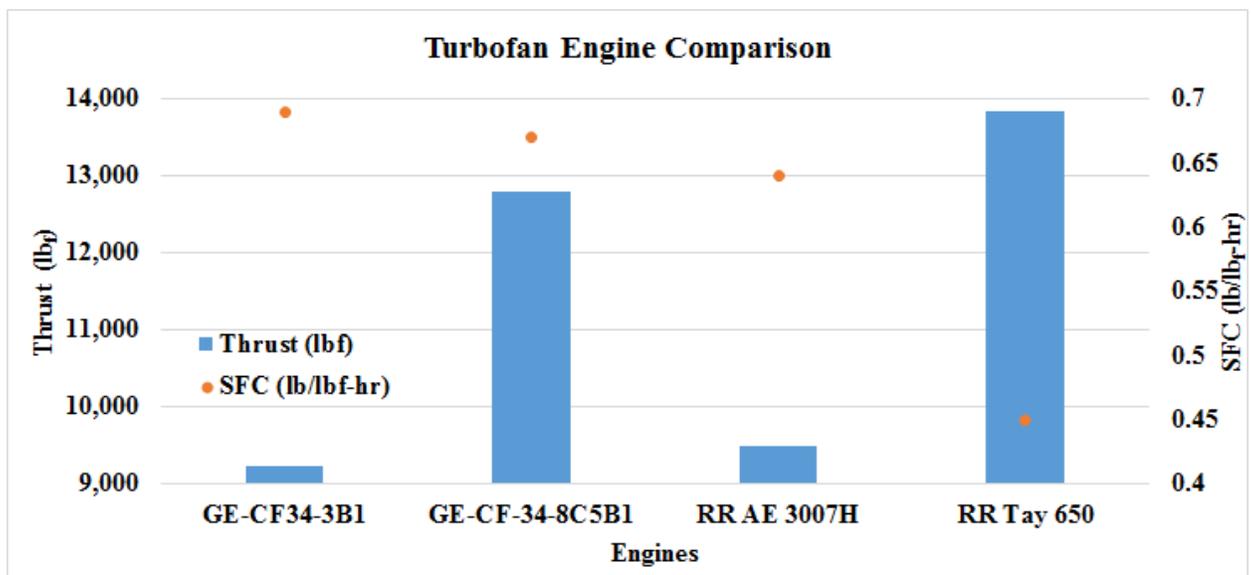
Figure 6.5-2 Turbofan Engine Thrust and SFC Comparison

7. Weight Breakdown

The empty weight breakdown is pertaining to the FF-1 Rainbird using fowler flaps with a Rolls Royce Tay engine at an aspect ratio of 6. The weight and center of gravity position of each component of the aircraft influences the balance and final maximum takeoff weight. Table 7-1 is a breakdown of the aircraft weight components.

Table 7-1 Empty Weight Breakdown Table for FF-1 Rainbird

Component	Weight (lb)	Component	Weight (lb)
Fuselage	4,080	Furnishings	1,290
Wing	4,660	A/C & Anti-Icing	120
Winglet	100	Avionics	1,000
Horizontal Tail	1,870	Payload Tanks	3,300
Vertical Tail	770	Pumps	1,000
Engines + Nacelles	6,970	Landing Gear	1,160
Fuel System	270	Crew	500
Surface Controls	960	**Total Weight**	**29,300**
Electrical System	1,300		

For the pie chart below in Figure 7-1, it displays the proportional percentage of the empty weight of the aircraft. With the fuel and payload added (59,200 lb), the maximum takeoff weight of the aircraft is 89,197 lb. Seen below of the empty weight breakdown that most of the weight lies on the engine and nacelles.
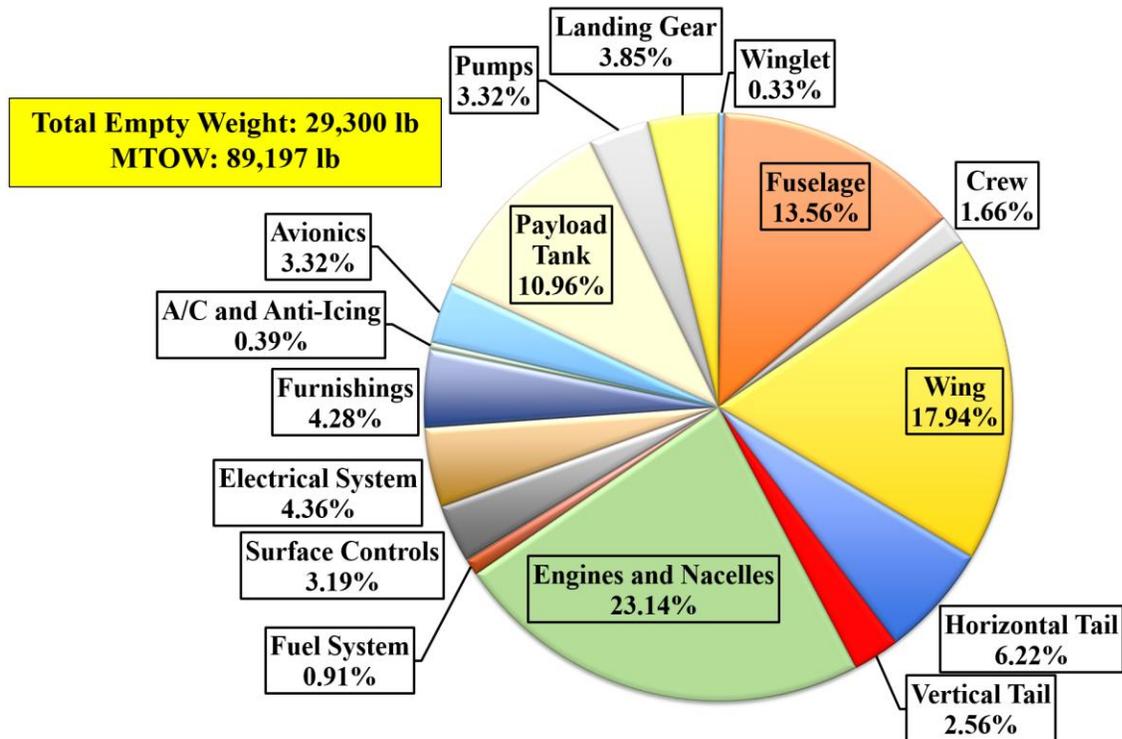
Figure 7-1 Empty Weight Breakdown of FF-1 Rainbird

7.1 CG Travel

The CG of each major component of the air tanker was determined first and expressed in terms of distance in feet from the nose. Then, each CG distances was multiplied by the weight of the corresponding component. Last, the sum of these products and the sum of the weights were implemented into the following equation:

$$X_{cg} = \frac{\sum x \times w}{\sum w}$$ **Equation 7.1-1**

The center of gravity of the FF-1 travels between 29.8% and 34.7% of the MAC under any loading configuration. The fire retardant and integrated tank have the largest influence on CG. In order to prevent falling outside of the recommended 25% to 35% MAC range, the wing and payload were placed accordingly. A 4.9% CG travel on a 19.7 ft MAC yields a maximum CG travel of approximately 0.97 ft.
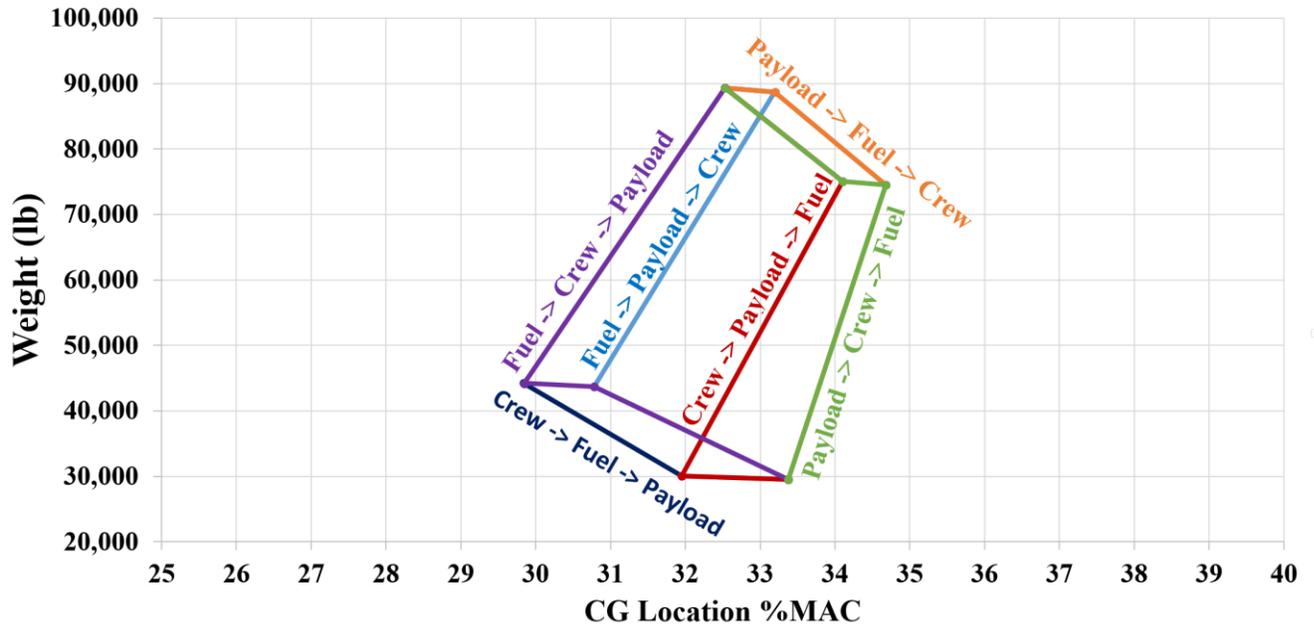
Figure 7.1-1 CG travel with respect to the leading edge of the Rainbird's MAC

8. Stability and Control

According to a statistical study of commercial jet airplane accidents published by Boeing in 2015 [13], there were a total of 29 airplane accidents in 2014. Of those 29 accidents, 2 were during takeoff and 21 were during landing. As the numbers show, takeoff and especially landing are the most crucial moments of air travel. The horizontal and vertical tails were sized according to weight distributions, CG, and one engine inoperative.

8.1 Vertical Tail Sizing and Analysis

The vertical tail design was started with the selection of the airfoil. The vertical tail airfoil selection was based primarily on symmetry. The N.A.C.A. 0012 was chosen due to its symmetry and its high lift coefficient. The airfoil has a lift coefficient of approximately 1.55, which is significantly larger than other four-digit airfoils such as the 0006 and the 0009 [1]. The increased drag for thicker wings is worthwhile for the vertical tail airfoil because the increase in drag is

surpassed by the increase in lift. Thus a strong lifting airfoil was chosen with a slightly high drag coefficient compared to thinner wings in order to produce strong yaw forces. A strong lifting airfoil allows the aircraft to be properly controlled without a large vertical tail. The most critical design factor in sizing the vertical tail is the scenario in which one engine becomes inoperative during takeoff. The FF-1's Rolls-Royce Tay 611-8 engines produce 13,850 lb of thrust each. Placed at a distance of 10 ft from the center of the fuselage, these engines would induce a moment of about 138,500 lb-ft in the event of one engine inoperative. By assuming the rudder was 42% of the vertical tail with a deflection of 30 degrees, the size of the vertical tail was calculated to be 180 ft² in order to counteract the moment caused by OEI. Table 8.1-1 contains all vertical tail dimensions.
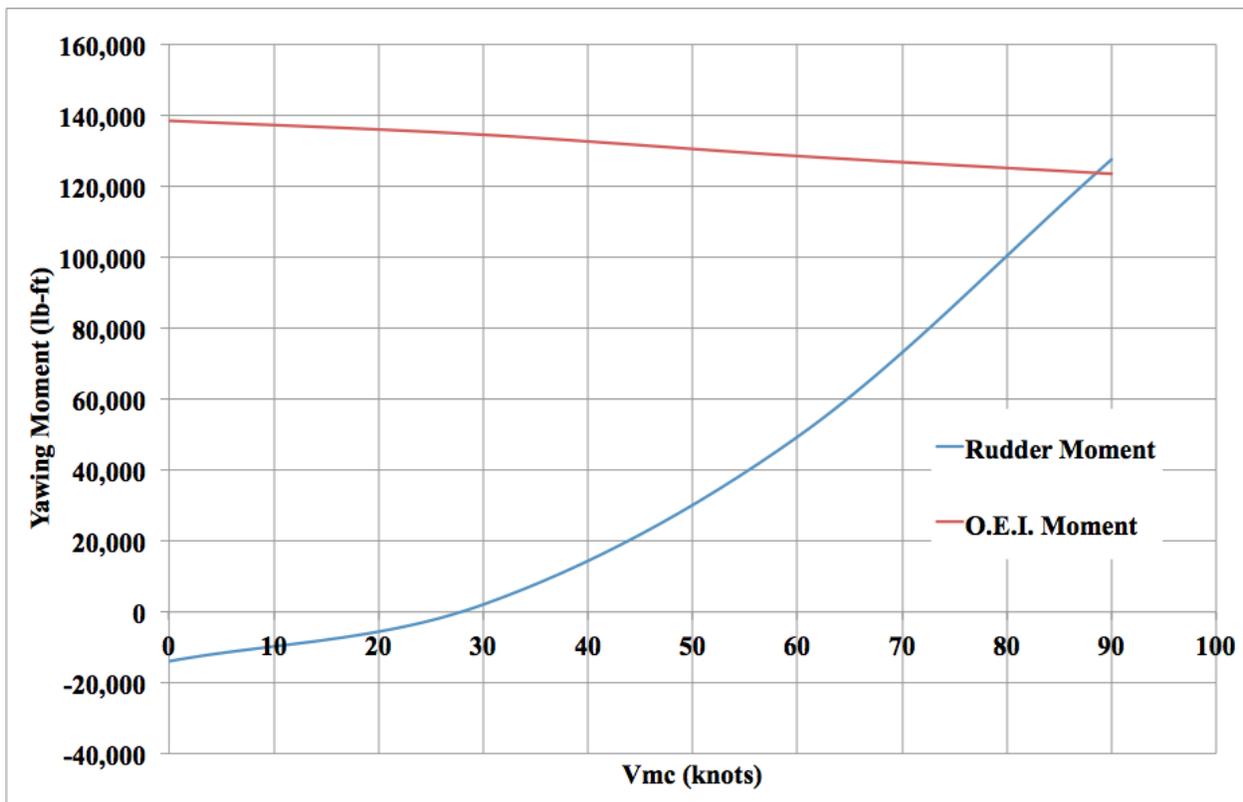
Figure 8.1-1: OEI Moment vs Rudder Moment

Table 8.1-1 Vertical Tail Parameters

Vertical Tail Parameters	
S_{VT}	180 ft^2
AR	1.2
Height	14.7 ft
Λ_{VT} @ 0.25 c	20°
Taper Ratio	0.8
Root Chord	13.6 ft
Tip Chord	10.9 ft
MAC Chord	12.3 ft
l_{VT}	28.5 ft

8.2 Horizontal Tail Sizing and Analysis

To design the horizontal tail, first the airfoil was selected using a similar method as the wing airfoil selection. The airfoil was chosen from N.A.C.A. airfoils using Abbott and Von Doenhoff's Theory of Wing Section.[1] As previously mentioned, four-digit airfoils have the least vulnerability to roughness and are optimized for low speed flight, thus the selection was narrowed down to four-digit airfoils. Since the 4415 airfoil was found to be a fitting choice for the large air tanker wing, the horizontal tail airfoil was chosen from the same family. The N.A.C.A. 4410 airfoil contains very similar aerodynamic characteristics to the 4415, and since the horizontal tail is not required to store fuel, a smaller thickness ratio is used to reduce drag. The N.A.C.A. 4410 airfoil has a maximum lift coefficient of approximately 1.6 and a parasitic drag value of approximately 0.0055. Once the airfoil was selected, it was possible to determine the volume tail coefficient. Upon constructing a notch chart, it was determined that the air tanker

would have a horizontal tail volume coefficient of 0.544. As a margin of safety, a horizontal tail volume coefficient of 0.55 was chosen to carry through calculations. Some of the prominent assumptions that went into the notch chart were a maximum deflection of 40 degrees and an elevator reference area ratio of 0.40.
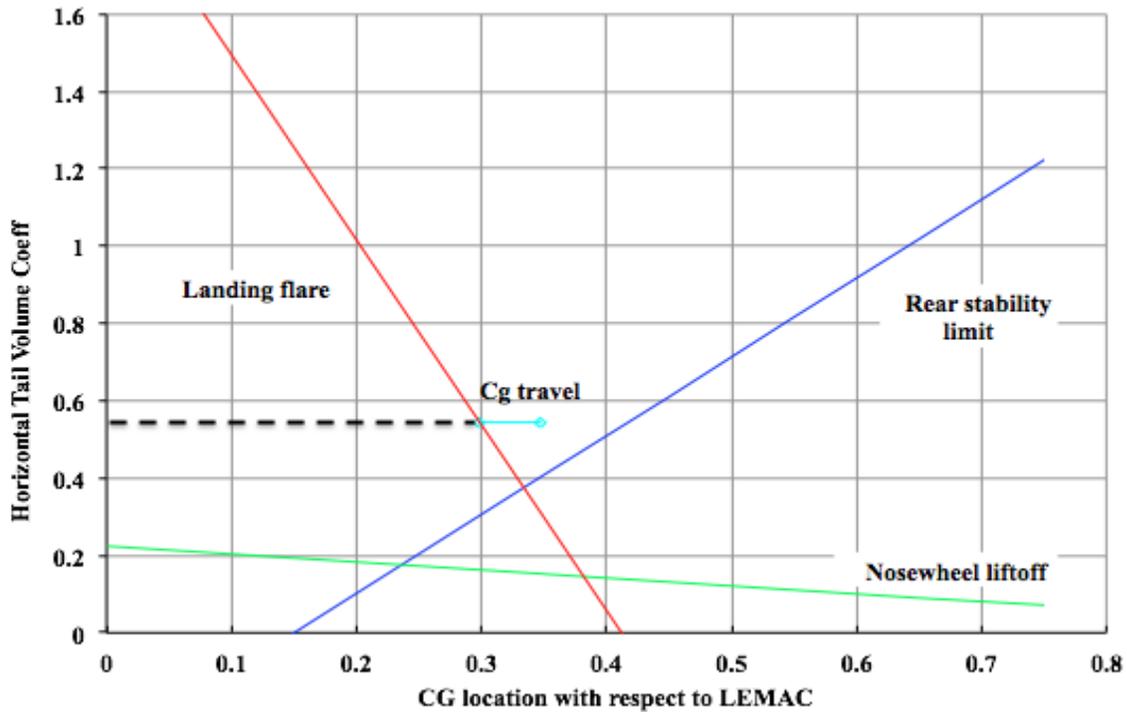
Figure 8.2-1: FF-1 Notch Chart

Table 8.2-1 Horizontal Tail Parameters

Horizontal Tail Parameters	
S_{HT}	746 ft^2
AR	4.5
Span	58 ft
Λ_{HT} @ 0.25 c	5°
Taper Ratio	0.45
Root Chord	17.8 ft

Tip Chord	8 ft
MAC Chord	13.5 ft
l_{HT}	30

The neutral point of the aircraft was determined in order to ensure static stability. The static margin is the distance between the CG and neutral point of the aircraft expressed as a percentage of the MAC obtained through Lab 8 Notes-Basic Aircraft Design Rules [9] using the following equations:

$$S.M. = (X_{np} - X_{cp})/c \qquad \textbf{Equation 8.2-1}$$

$$Vh = S_h l_h / Sc \qquad \textbf{Equation 8.2-2}$$

$$X_{np}/c = ¼ + [(1+2/AR)/(1+2/AR_h)*(1-4/(AR+2)]V_h \qquad \textbf{Equation 8.2-3}$$

The distance between the CG and neutral point is 3.57 ft and the static margin was determined to 0.18, making the Rainbird longitudinally stable.

8.3 Wing Control Surfaces

The type of flap utilized on the Rainbird was a major design variable. Four different flap types were included in analysis. The split flap was the least beneficial as it added the most weight and least amount of lift. The hinged and zap flaps added a balance of lift and weight. After many iterations, it was determined that the Fowler Flap would add the most lift to the air tanker with the least MTOW.

9. Aerodynamic Analysis

After determining the wing parameters from the continuous iterative process, aerodynamic parameters were calculated for the FF-1.

9.1 Drag Estimation Method

Using the method in <u>Elements of Aircraft Preliminary Design</u> the drag buildup of the FF-1 was found [13]. The drag buildup was performed for the cruise configuration with conditions to meet the dash requirement of 300 knots at the chosen cruise altitude of 20,000 feet. The total drag coefficient for the cruise configuration performed at various lift coefficients was calculated by adding the parasite drag coefficient, C_{Dp} and induced drag coefficient, C_{Di}. Equation 8.1-1 below shows the parasite drag equation from <u>Elements of Aircraft Preliminary Design</u> book [14].

$$C_{D_p} = \frac{f}{S_{ref}}, \text{ where } f = 1.1*(C_{wing} + C_{fuselage} + C_{vt} + C_{ht} + C_{winglet} + C_{nacelle} + C_{flap/slotted}) \quad \textbf{Equation 9.1-1}$$

The Oswald efficiency factor for the aircraft was also needed to determine the drag due to lift for various lift coefficient. Using the method in <u>Aircraft Design: A Conceptual Approach</u> as shown in equation 8.1-2 determined an Oswald efficiency of 1.113 [12].

$$e = 1.78 * (1 - 0.0045 * AR^{0.68}) - 0.64 \quad \textbf{Equation 9.1-2}$$

Table 8.1-1 list the individual components of the aircraft that were taken into account for the drag buildup with its drag count. The FF-1 has a total drag count of 140.

Table 9.1-1: Drag buildup at cruise Mach number of 0.45 at 20,000 feet.

Component	Drag Count
Wing	72
Winglet	1

Fuselage	30
Horizontal Tail	24
Vertical Tail	6
Pylons	1
Nacelles	4
Flap Hinges	2
Total	**140**

Figure 9.1-1 shows the drag polar calculated for the design using the equations from

Elements of Aircraft Preliminary Design [14]. A tangent line can be drawn from the origin to the

curve, where the intersection of the two lines represents the highest lift coefficient with the

lowest drag coefficient. As seen in Figure 8.1-1 this point corresponds to a lift coefficient of 0.6

with a drag coefficient of 0.0324.
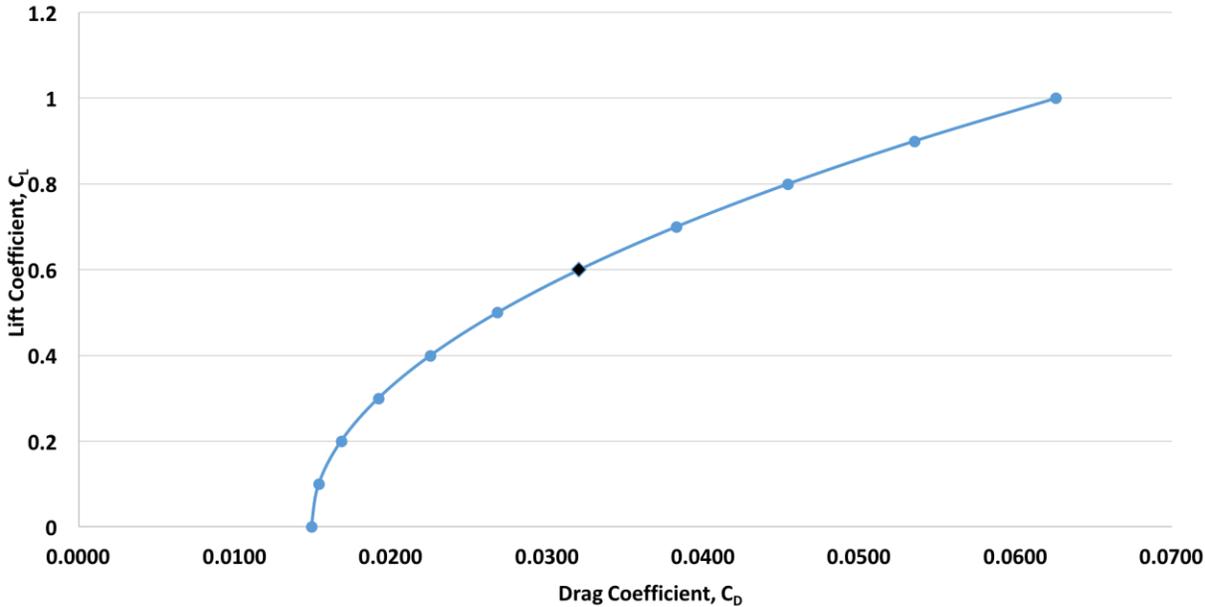
Figure 9.1-1: Drag Polar, Cruise Configuration

9.2 L/D

Using the parasite drag coefficient, C_{Dp} and induced drag coefficient, C_{Di} that was calculated before, the lift to drag ratios were then determined. Figure 8.3-1, shown below, graphically shows the L/D ratios. The maximum L/D for aspect ratio of 6 and taper of 0.4 was 19.4 at a lift coefficient of 0.6. This figure includes the 5% increase due to the winglets.
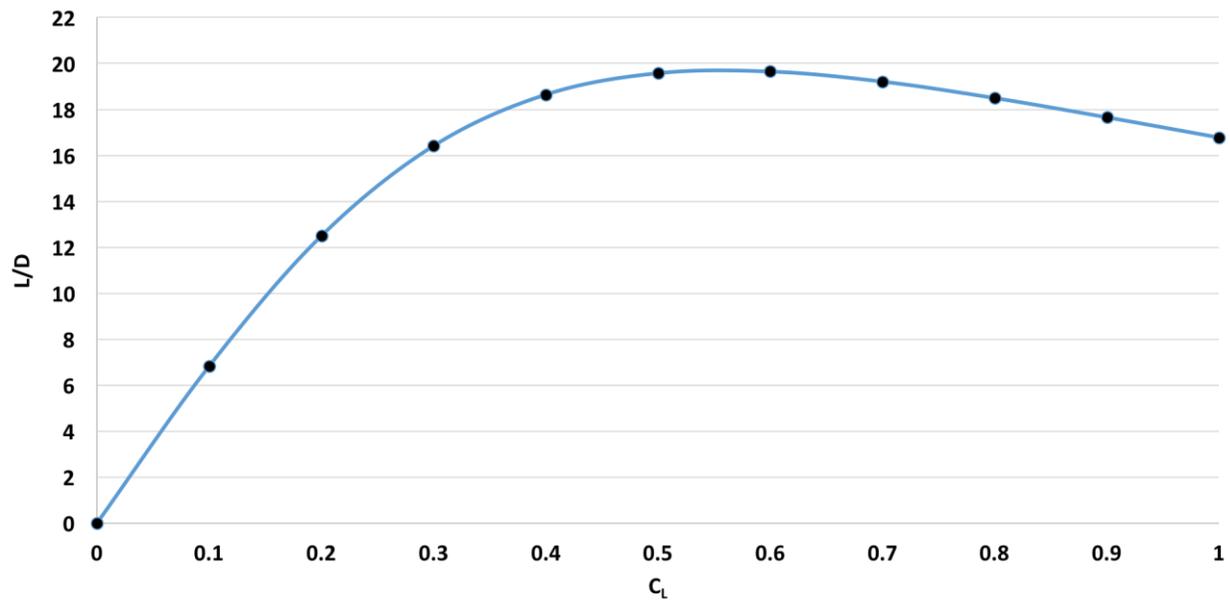
Figure 9.2-1: L/D Curve at Various Lift Coefficients

9.3 Low Speed Lift Curves

The C_{LMAX} values were obtained from the design point that met the RFP requirements of having an operational radius of 200 nm, 2,500 nm ferry range, balanced field length of 5,000 ft, stall speed of 90 knots, and dash speed of 300 knots. The calculations for the takeoff and landing C_{LMAX}, were taken from Schaufele's <u>Elements of Aircraft Preliminary Design</u> and Wood's <u>Aircraft Design</u> on C_{LMAX} increase based on the different types of flaps utilized in the aircraft [18]. In order to find the clean configuration of the low speed lift curve the following plots were used from Schaufele[14]:
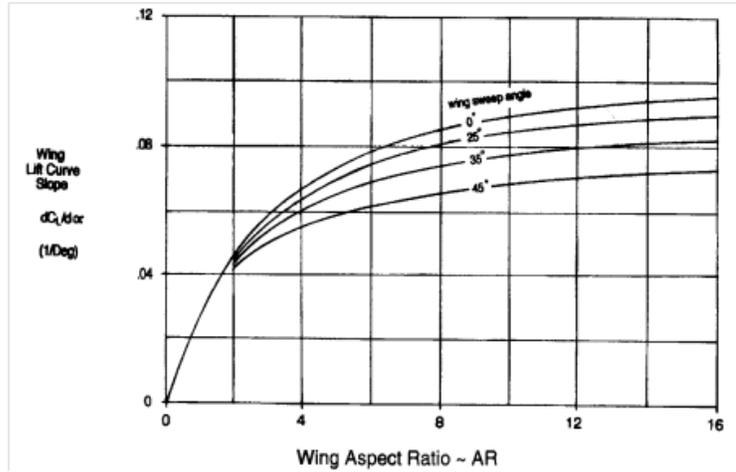
Figure 9.3-1: Lift Curve Slope Variation with Aspect Ratio and Sweepback
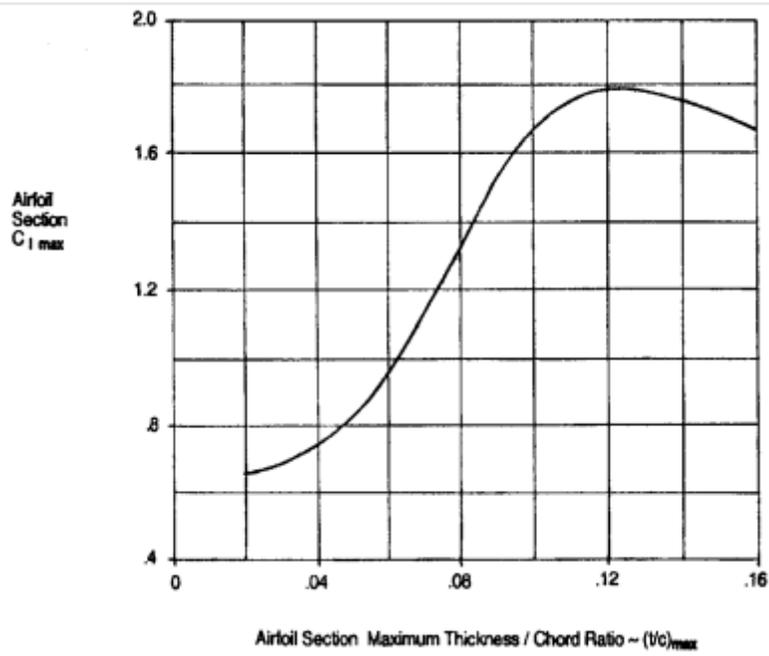
Figure 9.3-2: Airfoil Section C_{lmax} Trend with Thickness Ratio
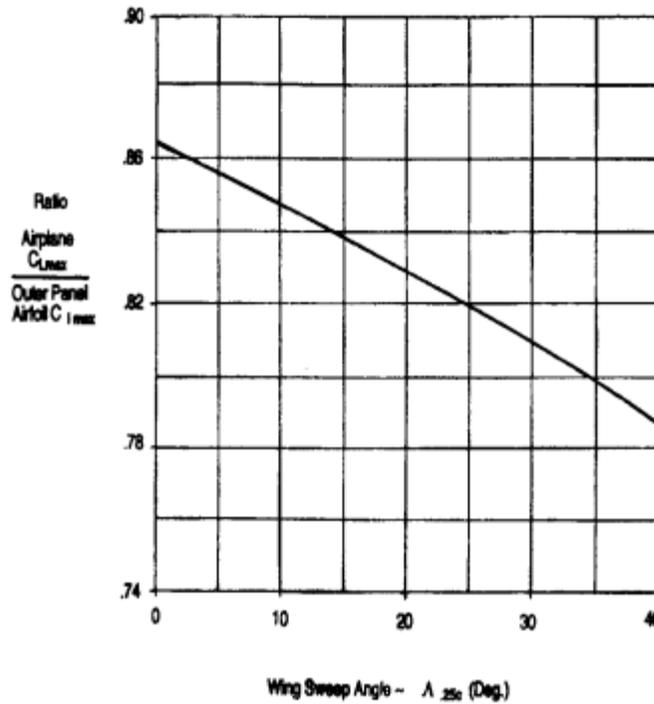
Figure 9.3-3: Airplane C$_{LMAX}$/Airfoil C$_{lMAX}$ Ratio

Figure 9.3-1, was used to obtain the lift curve slope of the aircraft, while 9.3-2 and 9.3-3

were used to get C$_{LMAX}$ of the aircraft. Once the lift curve slope was generated, the clean

configuration, takeoff, and landing were obtained through iteration. The lift lines can be seen in

Figure 9.3-5 respectively. Using the information obtained from Wood's book in Figure 9.3-4, the

lift curve slope was also extended for various types of flaps. The flaps analyzed are the split flap,

hinged flap, zap flap, and the fowler flap.

Type No.	Sketch	$C_L^{(1)}$ max.	C_{Dmin} Flap up	$-C_{Mo}^{(1)}$ Flap down	Wt. added	Min. Drag added	1st cost add.	Oper cost add.	Rel. chord const.V_s
1. Normal Wing		1.4	.010	.07	0	0	0	0	1
2. Split Flap		2.1	.010	.26	10%	2%	15%	1%	.67
3. Hinged Flap		2.2	.010	.30	5%	5%	10%	1%	.64
4. Hall Flap		2.2	.010	.29	12%	5%	15%	2%	.64
5. Zap Flap		2.4	.010	.40	12%	2%	20%	2%	.58
6. Flap and LE ailerons		2.4	.011	.22	15%	10%	20%	2%	.50
7. Fowler Flap		2.8	.011	.80	20%	10%	30%	5%	.50
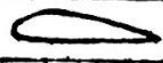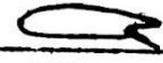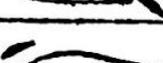
$$\underbrace{\frac{\Delta W}{W} \quad \frac{\Delta D}{D} \quad \frac{\Delta C_1}{C_1} \quad \frac{\Delta C_2}{C_2} \quad \frac{\Delta S}{S}}$$

Constant wing area

Figure 9.3-4: Flap Effects on C_{LMAX}

As such, the low speed lift curve for the Rainbird is shown in Figure 9.3-5 with an aspect ratio of 6. The C_{LMAX} for clean configuration is 1.46 thus making C_{LMAX} for landing is 2.47 and the C_{LMAX} for takeoff is 1.96. In order to obtain the C_{LMAX} values, the flap deflection angle for landing is at 40 degrees and for takeoff it is at 20 degrees. The C_{LMAX} values were obtained using fowler flaps as it added the most amount of lift with the least amount of weight onto the wings at 80% span of the wing and 30% of the chord.
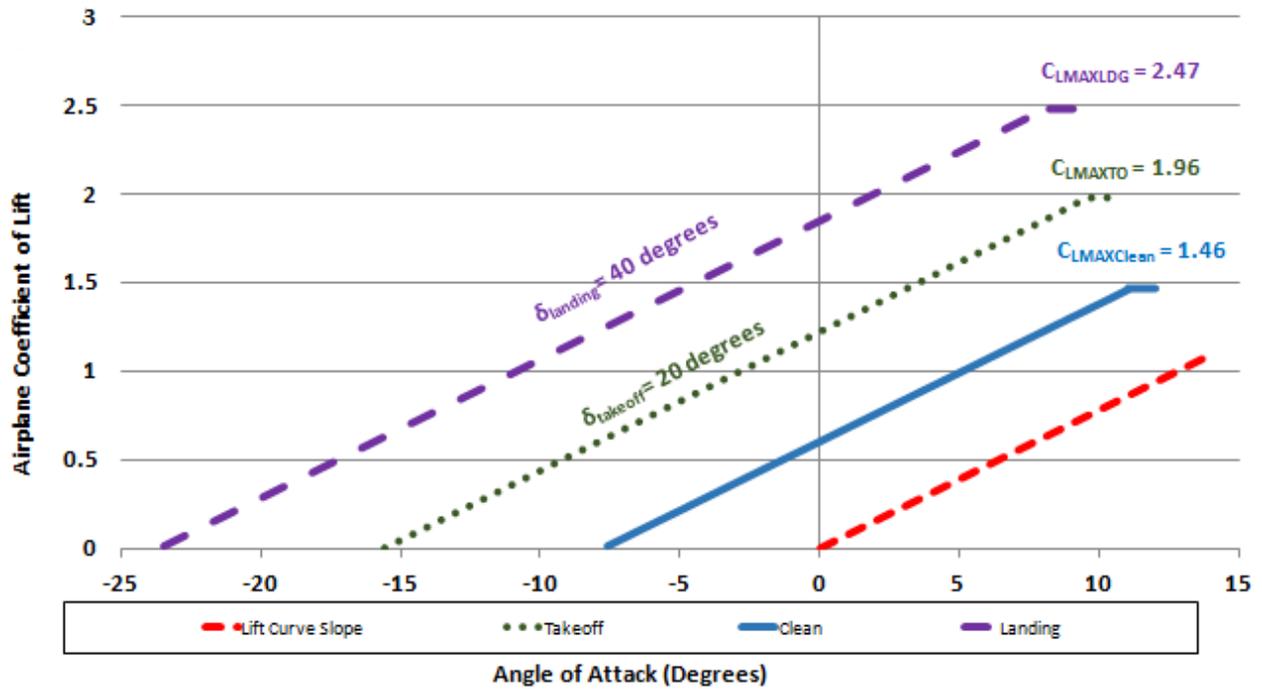
Figure 9.3-5: Low Speed Lift Curve for Fowler Flaps AR 6

10. Performance Analysis

Upon completion of the aerodynamic analysis, the performance analysis was completed to ensure that the Rainbird met all the RFP requirements.

10.1 Payload-Range

Carrying just enough fuel for one sortie is infeasible. The amount of time it takes to refuel the FF-1 in between sorties (30 min) far exceeds the required retardant reload time of ten minutes specified by the RFP. In order to meet this requirement, the FF-1 will carry enough fuel for four sorties. The FF-1 will also carry enough fuel to be able to travel 200 nm back to base in case the payload drops are unsuccessful on the last sortie. This results in 14,175 lb of fuel for the fire mission. The ferry mission will require 13,428 lb of fuel to travel 2500 nm. However, if the maximum fuel capacity (14,175 lb) is used, the FF-1 Rainbird is capable of travelling up to 2615 nm.

33

10.2 Balanced Field Length

The balanced field length of the FF-1 was determined using Schaufele's The Elements of Aircraft Preliminary Design. All engine acceleration, OEI acceleration, and rejected takeoff deceleration lines were plotted and integrated in order to graph accelerate-stop and accelerate-continue lines. The intersection of these two lines gives the balanced field length as well as the engine failure recognition speed. The Rainbird was determined to have a balanced field length of 3,793 ft.
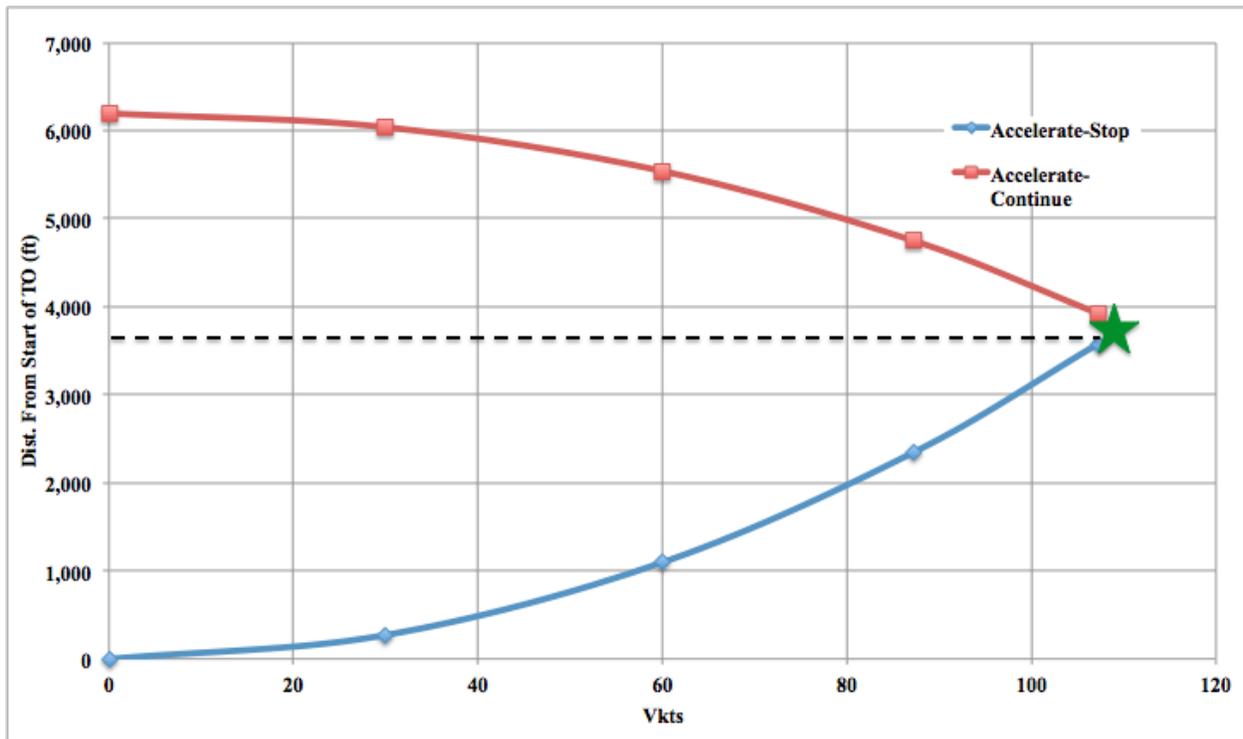
Figure 10.2-1: Takeoff Acceleration-Deceleration Chart

10.3 Optimal Cruise Altitude and Speed

The amount of fuel required, in lb, while establishing a fire line (four sorties) was determined for altitudes 10,000 ft- 30,000 ft above mean-sea-level, in increments of 1,000 ft. The calculation was repeated for four Mach numbers: 0.3, 0.35, 0.4 and 0.45. The amount of fuel was determined from the Breguet Range Equation. Table 10.3-1 identifies the most fuel efficient Mach number for each altitude by highlighting the fuel amount in yellow.

Table 10.3-1 Fuel and Time Required to Establish a Fire Line

Potential Cruise Altitude (kft)	M 0.3	M 0.35	M 0.4	M 0.45	Time to Reach Fire (min)
10	16,690	17,000	17,770	18,780	63
11	16,440	16,640	17,350	18,295	63
12	16,200	16,310	16,940	17,820	63
13	15,990	15,990	16,540	17,370	56
14	15,800	15,670	16,160	16,920	56
15	15,630	15,380	15,790	16,490	56
16	15,490	15,110	15,440	16,080	57
17	15,380	14,850	15,100	15,680	57
18	15,290	14,605	14,770	15,290	58
19	15,260	14,380	14,460	14,910	58
20	15,250	14,180	**14,175**	14,560	**54**
21	15,300	14,000	13,890	14,210	55
22	15,390	13,840	13,630	13,890	56
23	15,550	13,710	13,380	13,580	57
24	15,800	13,610	13,150	13,270	58
25	16,120	13,540	12,950	13,000	58
26	16,630	13,510	12,755	12,720	57
27	17,230	13,510	12,590	12,470	59
28	18,030	13,565	12,450	12,240	60
29	19,110	13,690	12,335	12,030	62
30	20,370	13,860	12,260	11,850	64
	Fuel Burned (lb)				

The time to reach a fire 200 nm away was then determined for the most fuel efficient Mach number for each altitude. The least amount of time (54 min) was obtained at a cruise altitude of 20,000 ft at a Mach number of 0.4 (245.6 kt). The time to reach the fire was determined from the rate of climb. The rate of climb for each altitude was found using Schaufele's method from the operational envelope [14]. The inverse of the rate of climb values for 10 kft, 15 kft, 20 kft, 25 kft, and 30 kft were plotted versus altitude in kft and the polynomial curve fit of Figure 10.3-1 was used to determine the time to climb for altitudes 10 kft-30 kft in increments of 1 kft by integrating the curve. This method is from *Introduction to Flight* [3].
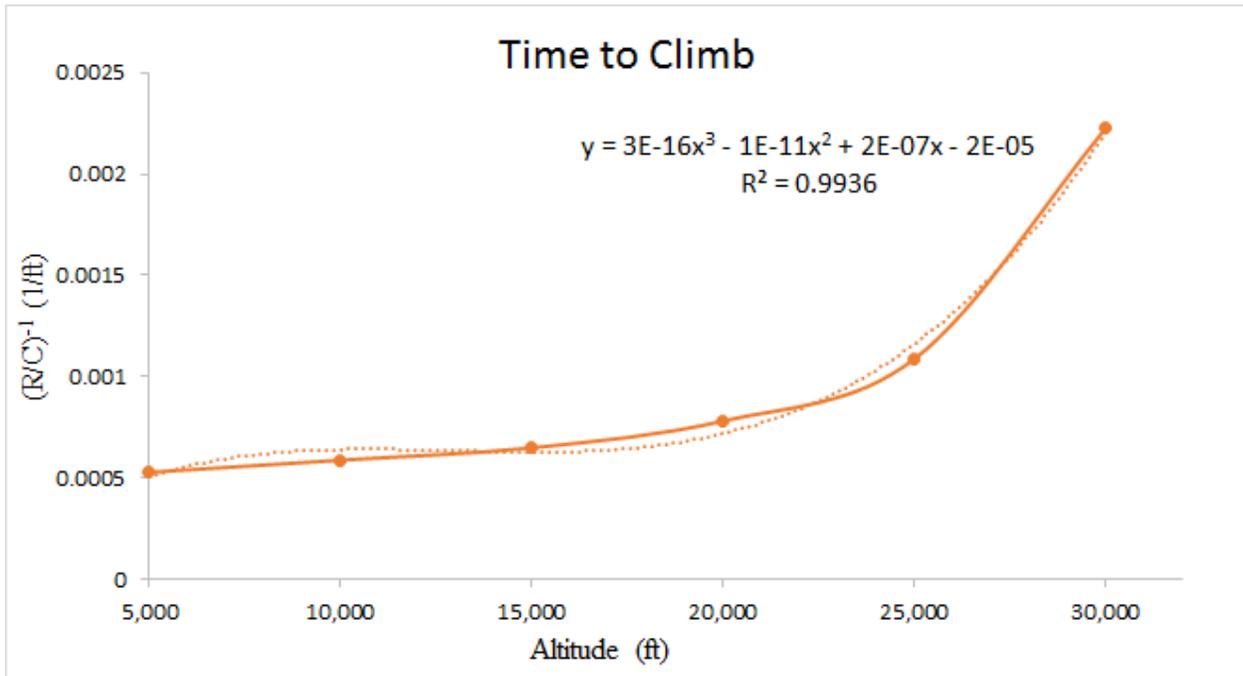
Figure 10.3-1 Polynomial Curve Fit of the Time to Reach Cruise Altitude

The Rainbird ascends to cruise altitude at a Mach number of 0.3. With the rate of climb and ascension Mach number known, the horizontal speed during climb was determined using the pythagorean theorem. Using the horizontal speed and time to climb, the horizontal distance traveled during the climb to cruise altitude was calculated. That distance was then subtracted

36

from 200 nm. The time to the remaining distance was determined from the potential cruise speed. The time to climb and the time to the remaining distance were summed to obtain the time to reach the fire.

10.4 Operational Envelope

An operational envelope was created for the FF-1 to show the different boundaries that the aircraft can operate under. The operational envelope is shown in Figure 10.3-1, the three boundaries in the operational envelope are the stall speed boundary, rate of climb boundary, and the thrust equals drag boundary. To determine these boundaries, Schaufele's Operational Envelope Method from chapter 13 was used [14]. An additional boundary was added to the operational envelope. This boundary is the speed the aircraft cannot operate due to the excess loads the aircraft would be experiencing. The stall speed was solved to be 89.98 kt. The chosen cruise altitude is 20,000 ft. with a cruise speed of 245.6 kt and dash speed of 300.4 kt. The aircraft is capable to dash at a maximum speed of 387 kt.
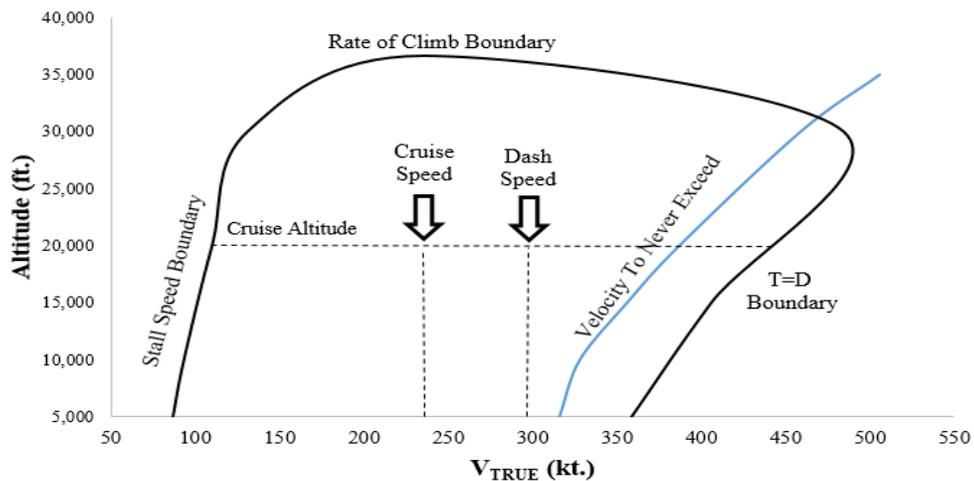
Figure 10.4-1 FF-1 Operational Envelope

11. Structural Analysis

The structural analysis for the aircraft began with the V-n diagram which was created using the Federal Aviation Regulations (FAR) Part 25 guidelines. Figure 11-1 is a plot of the V-n diagram with the cruise speed, stall speed, and maneuvering speed in knots. The V-n diagram was constructed using a mass take off weight of 89,197 lb.The gust factors are the lines shown in purple and is stated by FAR 25, that the "gust velocity may be reduced from 56 ft/s to 44 ft/s" from "sea level to 15,000 feet". Moreover, additional gust velocity may be "further reduced linearly from 44 ft/s to 26 ft/s" from "15,000 feet to 50,000 feet." The gust factors are shown in purple in Figure 11-1. The load factors range from -1 to 3.8 as required from FAR 25. What is shaded in green is the normal operating range of the Rainbird, while what is shaded in orange is the caution range. The V-n diagram shows that the Rainbird is more than capable of dashing at 300 knots as required by the RFP.
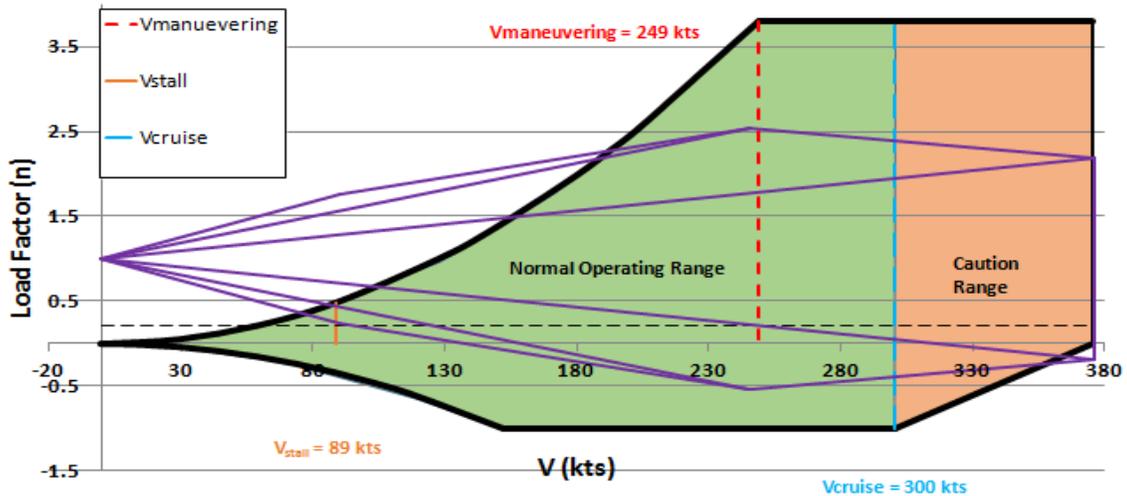
Figure 11-1: V-n Diagram

11.1 Wing Structure

With the highest load factor of 3.6 at 300 knots, the aircraft wing was modeled using

Desktop Aeronautics LinAir.
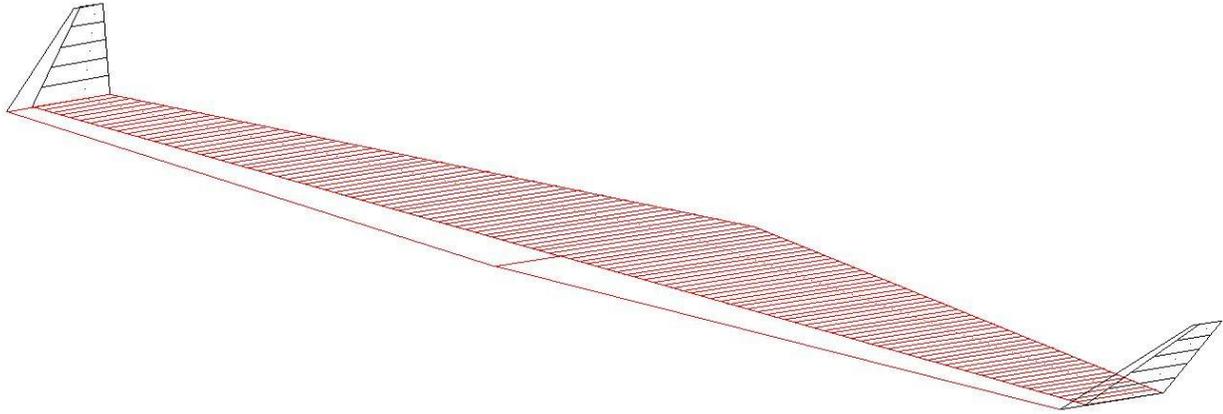
Figure 11.1-1 Wing With Winglets Modeled in LinAir

Through the use of panel methods in the program, the spanwise lift distribution was

found. This data was plotted in Excel to be in terms of spanwise load distribution incorporating

the weight of the wing, fuel, and the engines as shown in Figure 11.1-2.
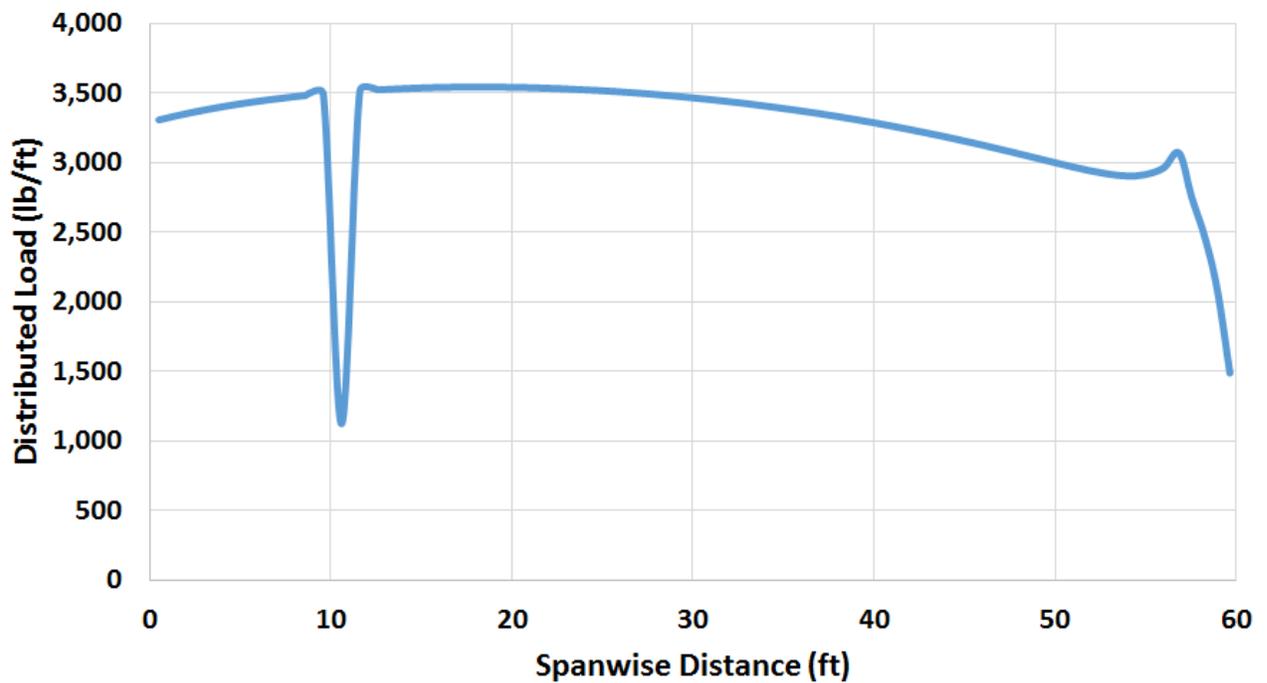
Figure 11.1-2 Spanwise Load Distribution

By integrating the plot of spanwise load distribution, the spanwise shear loading of the

wing was found and is shown in Figure 11.1-3.
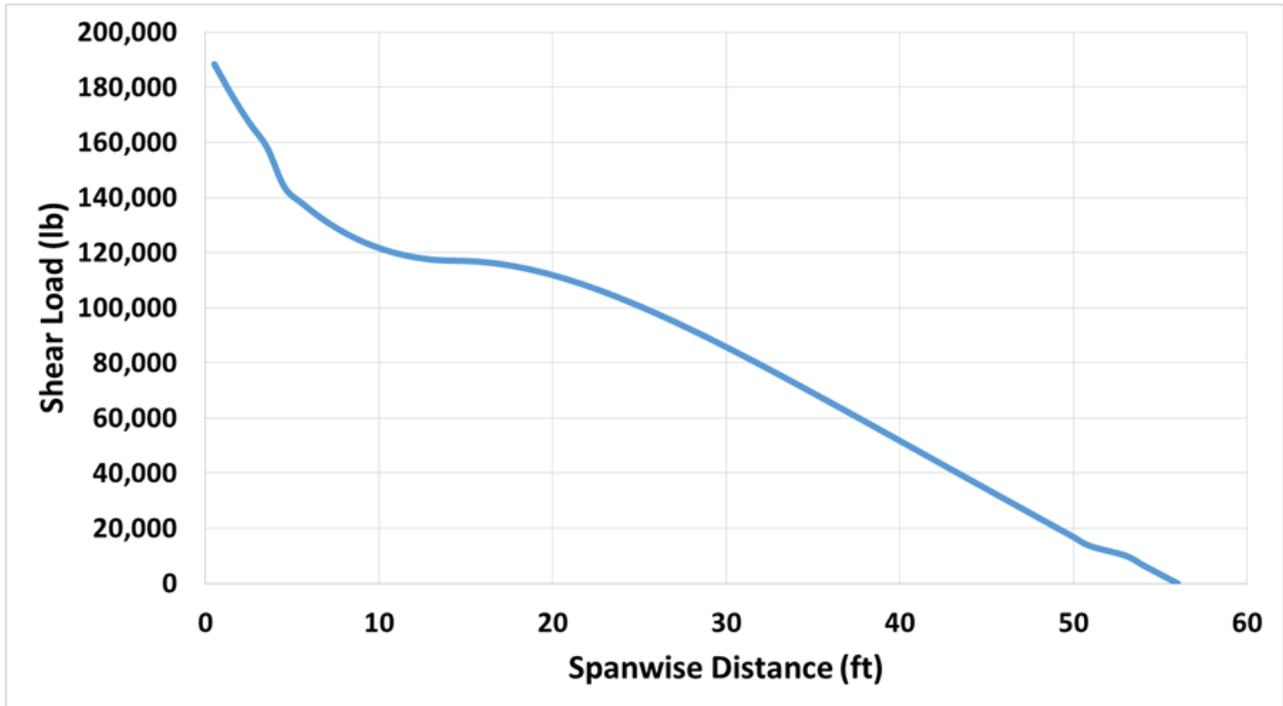
Figure 11.1-3 Spanwise Shear Load Distribution

The plot shows that the max shear load was at the root of the wing at 190,000 lb.

Integrating the shear load plot gives the spanwise bending moment of the wing shown in Figure

11.1-4.
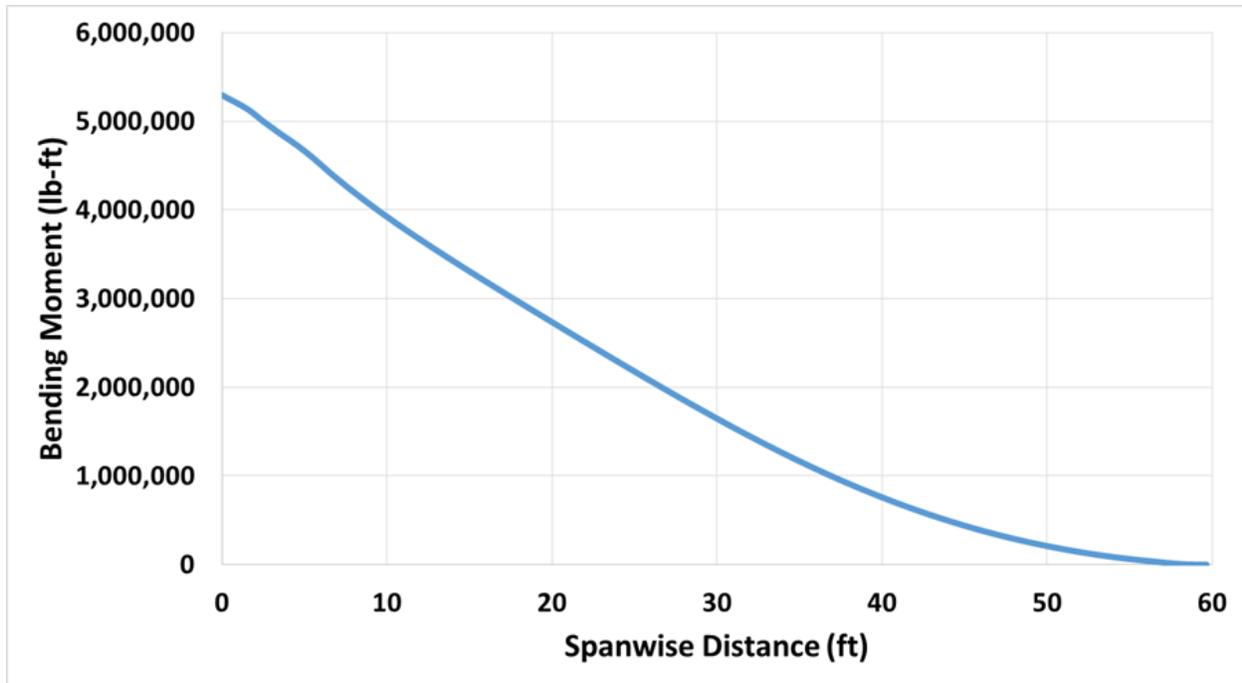
Figure 11.1-4 Spanwise Bending Moment Distribution

The plot shows that at the wing root, the wing experiences the highest bending moment 5.3 million lb-ft during the most extreme flight conditions. Since that is the highest load the wing will be subjected to, a 1.5 safety factor was applied to it and used to create the wing structure.

Using the methods in Bruhn, an Excel table was set up to find the max bending and loads on the spars and stringers utilizing their moments of inertia and effective areas with the wing skin.[4] The wing utilizes 3 spars, located at 20%, 60% and 70% of the wing chord, 13 hat stringers on the upper wing skin, and 13 L stringers on the lower wing skin. The effective areas of the T, Hat, and L sections are 1.5, 0.356, and 0.23 in^2 respectively.

The material selected is aluminum 7050-T7451 due to its great combination of strength, stress corrosion cracking resistance, toughness and fatigue resistance. By varying the sizing and locations of the wing components the max loads that they each experience were found. The max loads were compared to the possible failure modes; crippling, Euler buckling, and inner-rivet

buckling. The wing structure was sized so that the aircraft will not fail during its 20+ year lifespan. The highest load is experienced on the spars and shown in Table 11.1-1.

Table 11.1-1 Spar Stress Analysis

Al 7050-T7451	
Yield Strength (ksi)	68
Max Load (ksi)	33
Crippling Allowable (ksi)	64
Margin of Safety	0.94

The ribs were also made of aluminum 7050-T7451. They are spaced 30 inches apart and are 0.08 inches thick. The resulting wing structure with the spars, ribs, and stringers is shown in Figure 11.1-5.
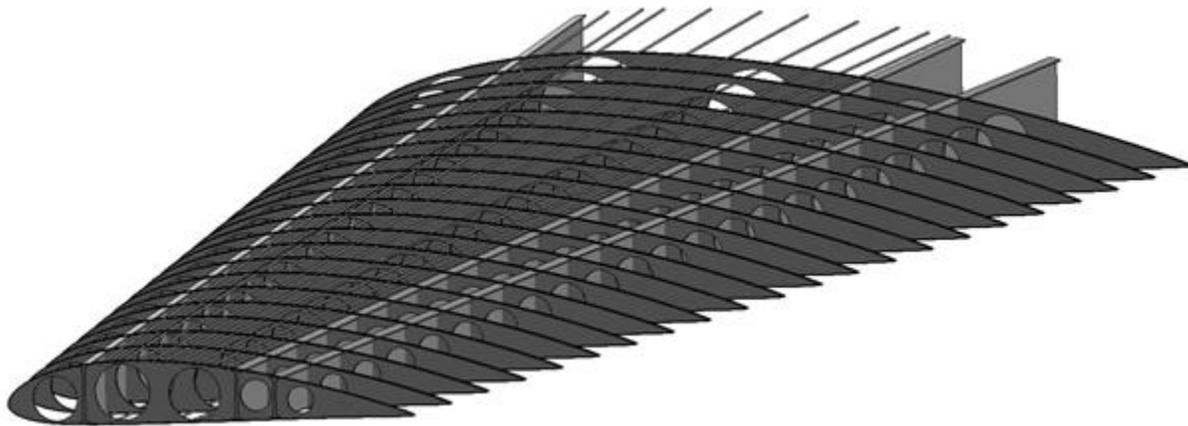
Figure 11.1-5 Wing Structure

11.2 Fuselage Structure

The fuselage of the aircraft is made up of Al 7050-T7451 frames, stringers, and bulkheads for the same reasons as it being used on the wing structure. The frames are spaced 10 inches apart in cabin and tail sections, that is the first 10% and last 20% of the fuselage length.

The main section of the fuselage has frames spaced 20 inches apart. In addition to the frames, there are bulkheads located at the end of the pressurized cabin section and at the location where the main wing attaches to the fuselage. The fuselage structure is shown in Figure 10.2-1 and the entire aircraft structure is shown in Figure 10.2-2.
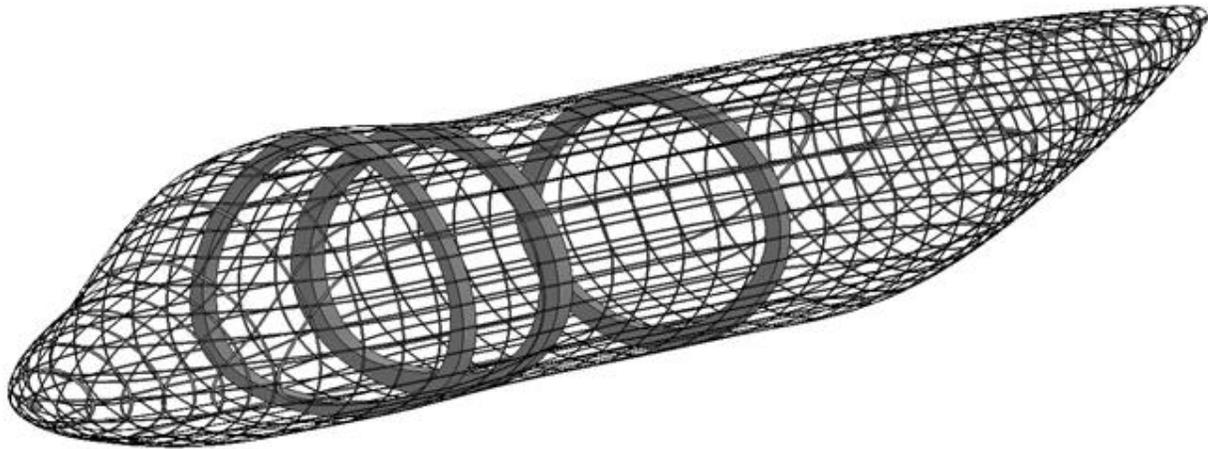
Figure 11.2-1 Fuselage Structure
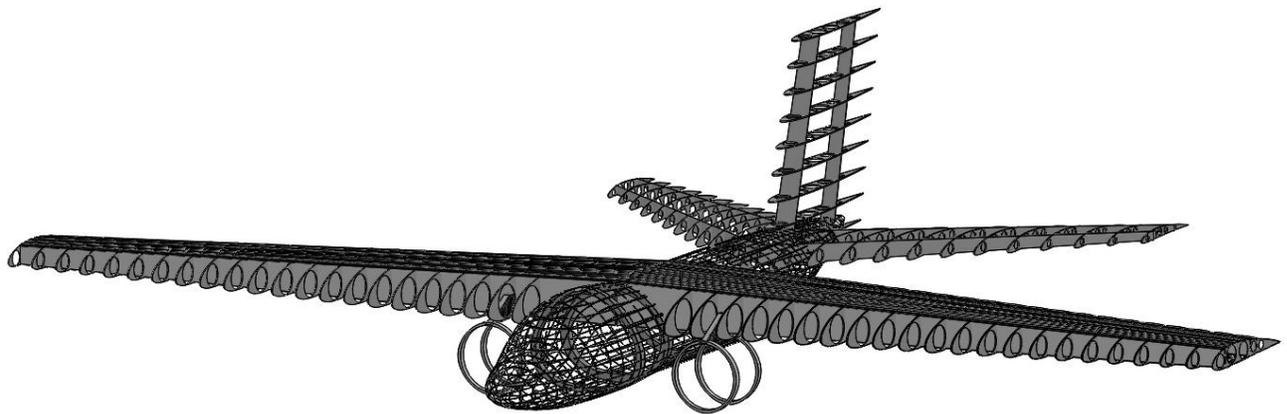
Figure 11.2-2 Aircraft Structure

11.3 Fatigue Analysis

In order for the aircraft to have at least a 20 year lifespan, fatigue stresses must be addressed. The aircraft designed for an assumed worst case lifetime; that is 1 fire a day

consisting of 4 missions per fire and 4 fully reversed cycles per mission. Across a 20 year span, that is 116,000 cycles.

To meet the 20 year operating requirement, the Modified Goodman Method from Shigley was used [15]. Thus the sizes of the internal structure, that is spars and struts as mentioned before were designed to have a maximum stress of 33 ksi and minimum stress of -4 ksi on a standard mission. These values were used to find the equivalent fully reversed stress and the finite fatigue lifetime of 177,000 cycles. Which is more than enough to meet our expected cycles experienced in 20 years with a margin of safety of 0.5.

12. Landing Gear

The landing gear for the FF-1 chosen was a retractable tricycle configuration. The gears were chosen to be retractable in order to decrease drag on the aircraft. The main gear stows away in pods on the side of the fuselage due to the limited space in the fuselage due to the payload tank, and not in the wings since the FF-1 has a high wing design and the added weight would not be feasible. The nose gear is shown in Figure 12-1 and the main gear is shown in Figure 12-2.
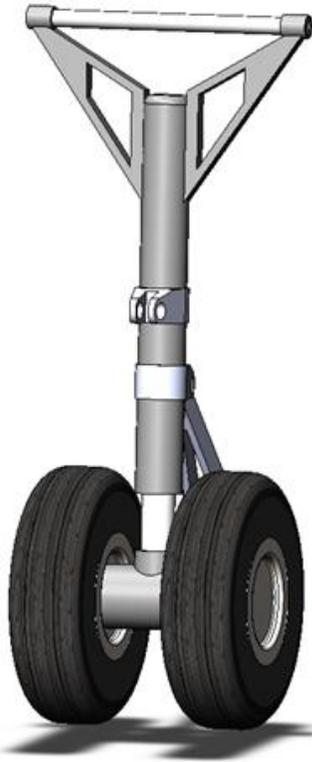
Figure 12-1 Nose Landing Gear

Figure 12-2 Main Landing Gear

12.1 Landing Gear Placement

The landing gear was placed in order to meet the minimum tip-back and tip-over angle requirements, and to prevent scraping of the tail on tip-back on take-off. The tip-back angle is 15.7 degrees.

The main gear is placed 2.6 feet aft of the aircraft center of gravity in order to carry the majority, 88%, of the load upon landing. The nose gear is placed 18.5 feet forward of the aircraft center of gravity carrying 12% of the load, this is done so that there is enough weight on the nose to easily turn while taxiing as well as not too much weight to prevent the aircraft from rotating during take-off.

Using the methods in Raymer, the loads that the landing gear experiences were calculated using statics to find the static loads [11]. The dynamic loads such as the braking load on the nose gear and the take off load on the main gear were found with the assumptions of a -3m/s^2 braking deceleration and a 4m/s^2 acceleration during takeoff respectively. The static and dynamic loads summed and then a 7% increase was added as FAR 25 requires.

12.2 Oleo Strut Sizing and Tire Selection

With the known locations and loads on the landing gears, tires were selected that can handle the loads. The tires selected were GoodYear Type VII tires with the 2 on the nose gear rated to 12,800 lb and the 4 on the main gear rated to 26,800 lb [7]. Type VII tires were chosen due to it being the standard tire choice on modern aircraft due to their conventional sectional shape and high load capabilities.

Due to the size and weight of the aircraft, the landing gears use oleo-pneumatic shock absorbers (oleo), which combines a mechanical coil spring with a hydraulic damper. The oleos

were sized using the methods in Raymer with an internal pressure of 1800 psi and a 10 inch

stroke length [10]. The resulting sizes are shown in Table 12.2-1

Table 12.2-1 Oleo Strut Sizes

	Diameter	in
	Nose	5.6
External	Main	7.9
	Nose	3.9
Internal	Main	5.5

13. Subsystems

Various subsystems were utilized in the FF-1 such as the fuel system, the cabin

pressurization and air conditioning to provide comfort to the pilot, and sensors to provide the

pilot with situational awareness.

13.1 Fuel

The FF-1 will carry 14,175 lb of fuel to complete its mission of a three drop sortie and

complete a total of four sorties to establish a successful fire line. The tank geometry will conform

to the shape of the wing with the utilization of a wet wing design. In addition, the internal

structure of the wing such as the ribs will mitigate the sloshing effects of the fuel during flight.

13.2 Cabin Pressurization and Air Conditioning

Due to the aircraft ascending and cruising to 20,000 ft, the aircraft will need supplemental

oxygen, cabin pressurization, and air conditioning to keep the pilot comfortable and prevent the

possibility of succumbing to hypoxia. The three systems will be limited to the cockpit due to it

being the only personnel room and the payload exploiting gravity as a means of dispersal [5].

The air conditioning and pressurization will utilize the engine bleed air system while in flight. To

address the oxygen demand, a pair of diluter-demand automatic pressure-breathing regulators

will be used in combination with LOX tanks with a 25 Liter tank providing up to 96 hours of oxygen, each.

13.3 Sensors

The aircraft will utilize two forward cameras that will grant the pilots of the FF-1 a complete view of the ground [8]. The cameras that will be used are the FLIR Systems MD-324 (Shown in Figure 13.3-1) which are capable of thermal imaging and are easy to mount. Each unit will cost $4200 with a combined cost of $8400 per aircraft.

Figure 13.3-1: FLIR Systems MD-324

14. Manufacturing Process

The manufacturing approach will undergo through several outsourced subsystems and systems to be built in-house. Some of the aircraft's components such as the wings, stabilizers, fuselage, and control surfaces will be manufactured in-house due to the due to proprietary design and intellectual property. The rest of the aircraft's components will be provided by subcontractors such as the following: engines-Rolls Royce Tay, retardant dispersal control system-Trotter Controls, camera sensors-FLIR Systems MD-324, and landing Gear tires-GoodYear Type VII

For the manufacturing process, the aircraft will go through six stages as shown in Figure 14-1.
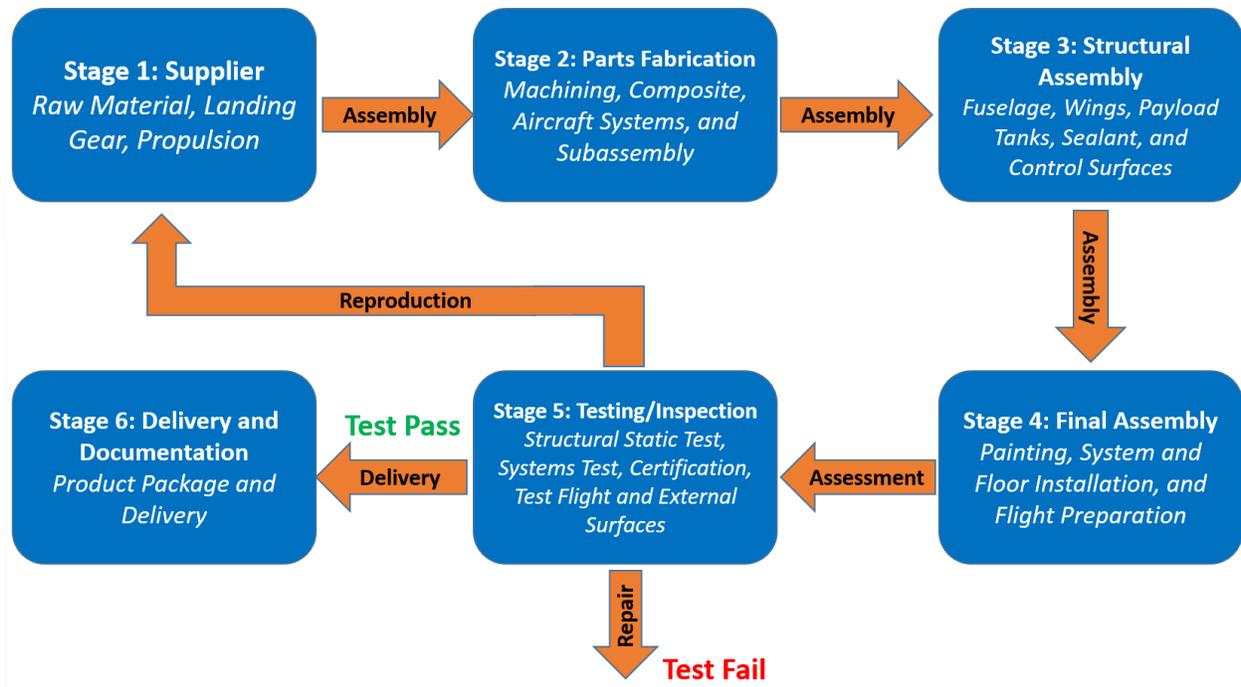
Figure 14-1: Manufacturing Process of FF-1 Rainbird

The first stage supplies the raw material and equipment to design and shape the aircraft. Stages 2-4 will continue the assembly of the aircraft with fabrication, structural assembly, and final assembly. Following the 4 stages of assembly, the aircraft will run through several tests and inspections using integrated test benches in order for the aircraft to be at the highest quality and performance. If the aircraft fails the test, it will return to the factory for repair; if the aircraft passes the test, it will move on to the next stage. After ground testing and test flights have been performed, the aircraft will undergo delivery and documentation as the final stage. With the reproduction, the assembly line method will ensure that the customers will continue to get their product at a timely matter.

15. Maintenance Process

The aircraft will be maintained by professional maintenance engineers and mechanics at a FAA approved repair stations under Title 14 of the Code of Federal Regulations (14 CFR) Part 145. The repair station will offer a wide variety of maintenance, repair, and overhaul (MRO) services which will include the airframe, power plant, engines, radio, instruments, dispersal system, and accessory components of the aircraft. The engine maintenance will cover full restoration, test cell runs, conditioning, trend monitoring, and non-destructive testing. Due to its simple and low maintenance design, the dispersal system check will be performed through fire gates beneath the aircraft as well as through the rear access door. Onboard diagnostics provided by the FRDS Gen II will also assure that the system is functioning properly, however routine maintenance will be done at the same time as aircraft and engine checks to guarantee system effectiveness. In order to best regulate the functionality of the aircraft, the FF-1 Rainbird will go through "A Check" maintenances. The "A Check" is a maintenance check performed either every 400-600 flight hours or every 200-300 cycles, whichever occurs first. This will ensure the aircraft will be at peak performance without the added risk of having structural or operational failures during flight.

16. Program Lifecycle
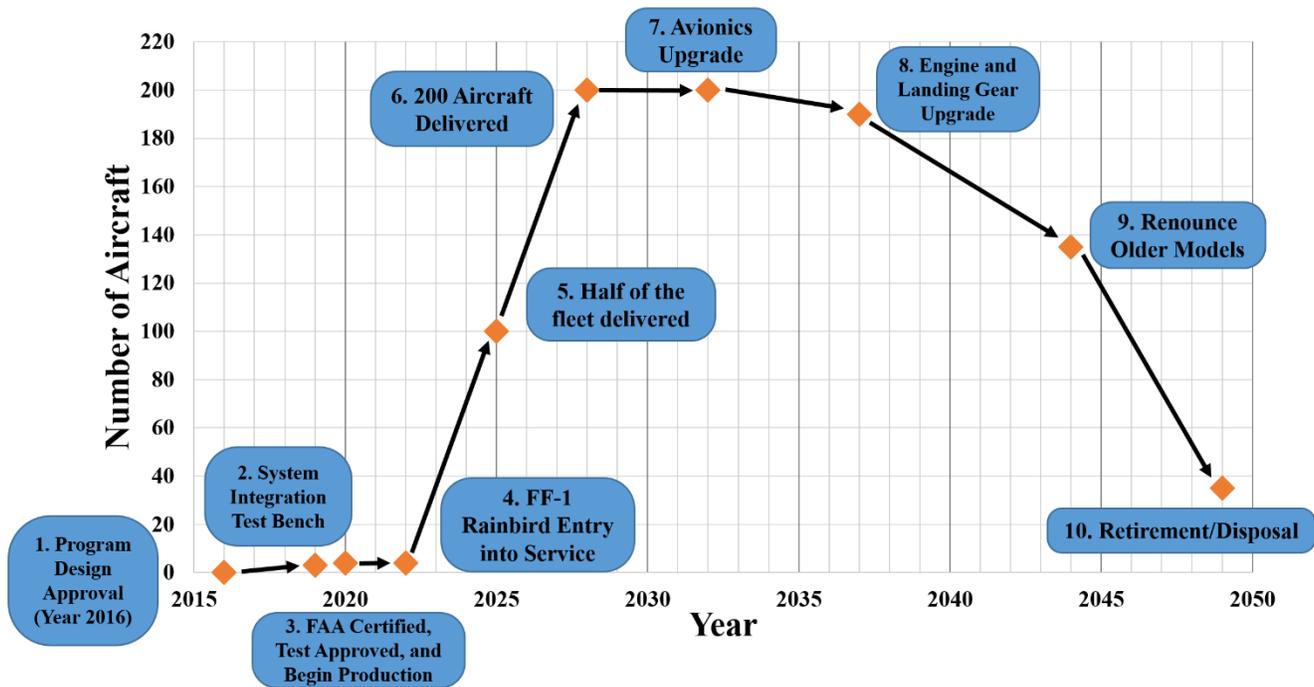
Figure 16-1: FF-1 Rainbird Program Lifecycle

To manage the construction and expectancy to ensure timely and accurate production process, the program's lifecycle of the aircraft will experience 10 primary milestones, as seen in Figure 15-1. With the first milestone, the program design approval is scheduled for July 2016. By 2019, the aircraft will undergo numerous full-scale testing such as the structural analysis, dispersal system, engine cell runs, and flight controls. By 2020, the program is expected to pass FAA certification tests, system integration tests, and begin the production of the aircraft in the assembly line. The FF-1 Rainbird date of entry of service will start in 2022, where the first fleets will be delivered to customers. With the production of 3 aircraft per month, half of the fleet production will be delivered by 2025 and then the entire fleet by 2028. Thereafter, there will be

scheduled upgrades which includes the avionics, engines, and landing gear to ensure the life

expectancy will continue until retirement in the year 2049.

17. Cost Analysis

The main goal of our large air tanker design is to minimize cost of ownership therefore,

to be less expensive than retrofitting, buying, and operating a current aircraft. Our target

customers are the ten fire regions across the United States. Each region will initially be sold four

aircraft and eventually buy another four sets to operate for 100 years. In addition, three

additional aircraft will be produced for RDT&E purposes.

Most costs were found using Nicolai and Carichner's cost method and will be specified

regardless.[11] To estimate the various costs, the aircraft's empty weight was solved for by

iterating for MTOW and using maximum speed and production quantity in combination. Due to

the aircraft availability being in 2022, all costs will be inflated to the aforementioned year using

the following equation

$$X_{inflated} = X_{current} * 1.031^{(\text{inflated year-current year})} \qquad \textbf{Equation 17-1}$$

Where $X_{inflated}$ is the inflated cost and $X_{current}$ is the pre-inflated cost.

17.1 Research, Development, Test, and Evaluation

The total Research, Development, Test, and Evaluation (RDT&E) costs for the FF-1

program was estimated to be $1.89 billion [10]. The RDT&E will include the cost of testing

three aircraft and was evaluated using Nicolai and Carichner's cost method. Figure 17.1-1

elaborates on the breakdown of the RDT&E costs.
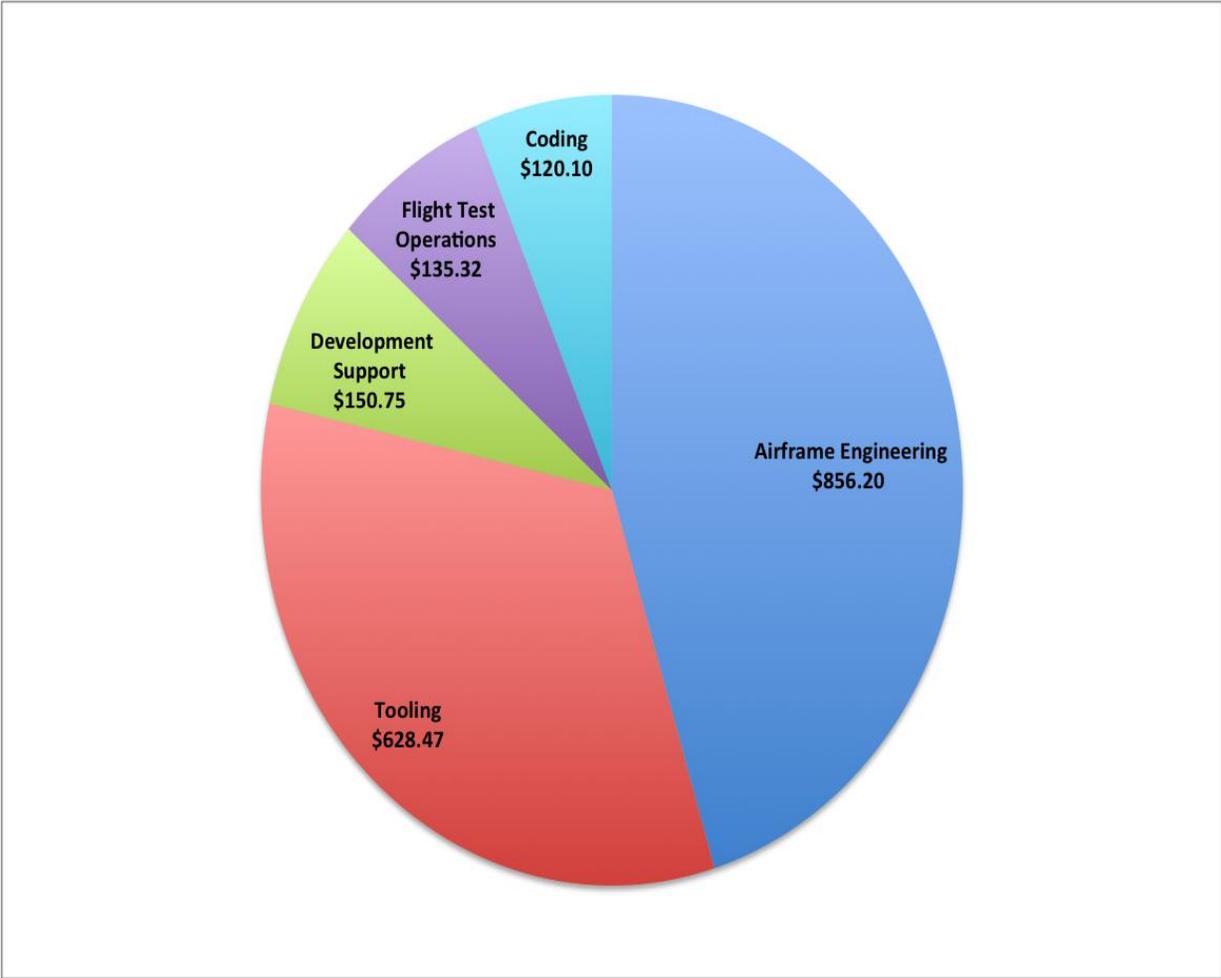
Figure 17.1-1: Research, Development, Test, and Evaluation Cost Breakdown ($ million)

17.2 Production Cost

The total production cost using Nicolai and Carichner's cost method was assessed to be $8.9 billion inflated to 2022 dollars.[10] Figure 17.2-1 displays the production cost breakdown in greater detail.
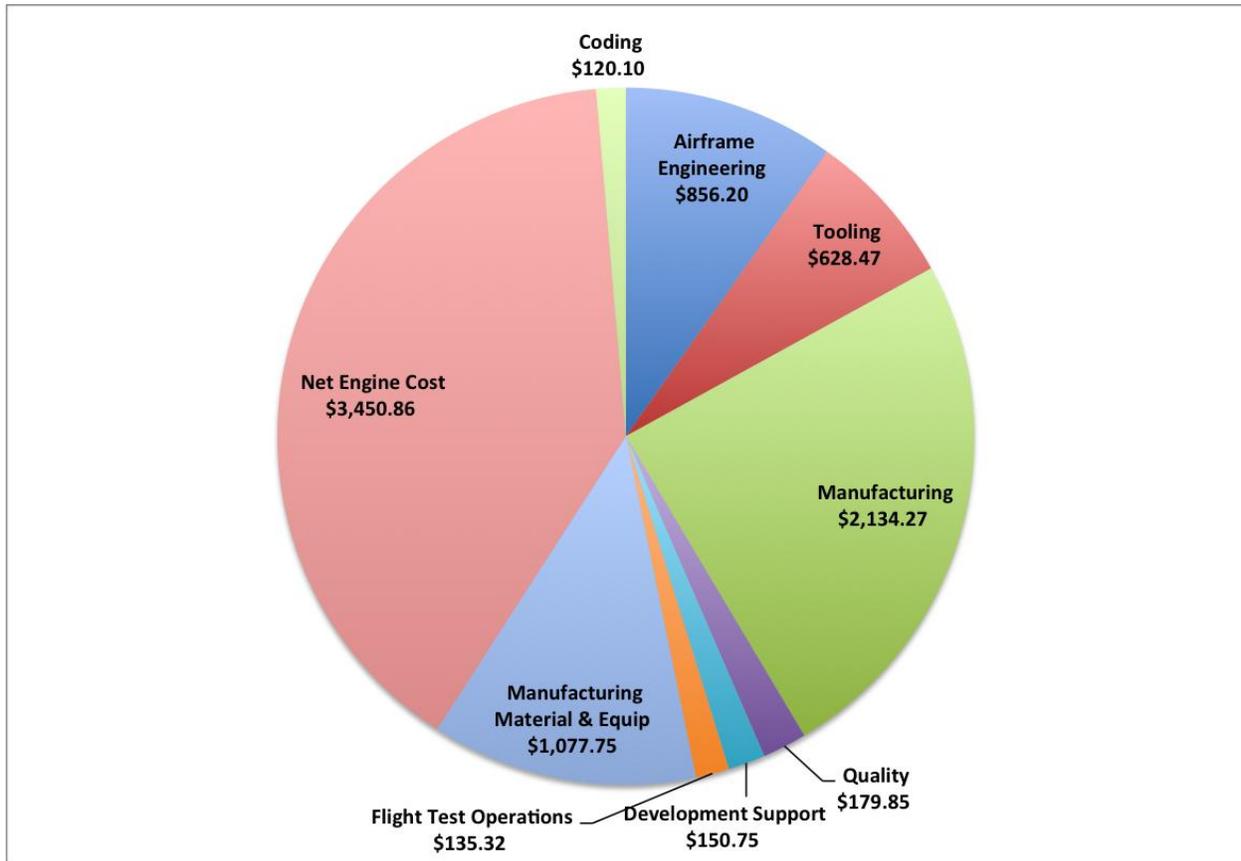
Figure 17.2-1: Production Cost Breakdown ($ million)

The total production, including the three test aircraft, will be 200 units. At 131 units, the program will break even in costs and begin to receive profit. Figure 17.2-2 illustrates the production break-even plot.
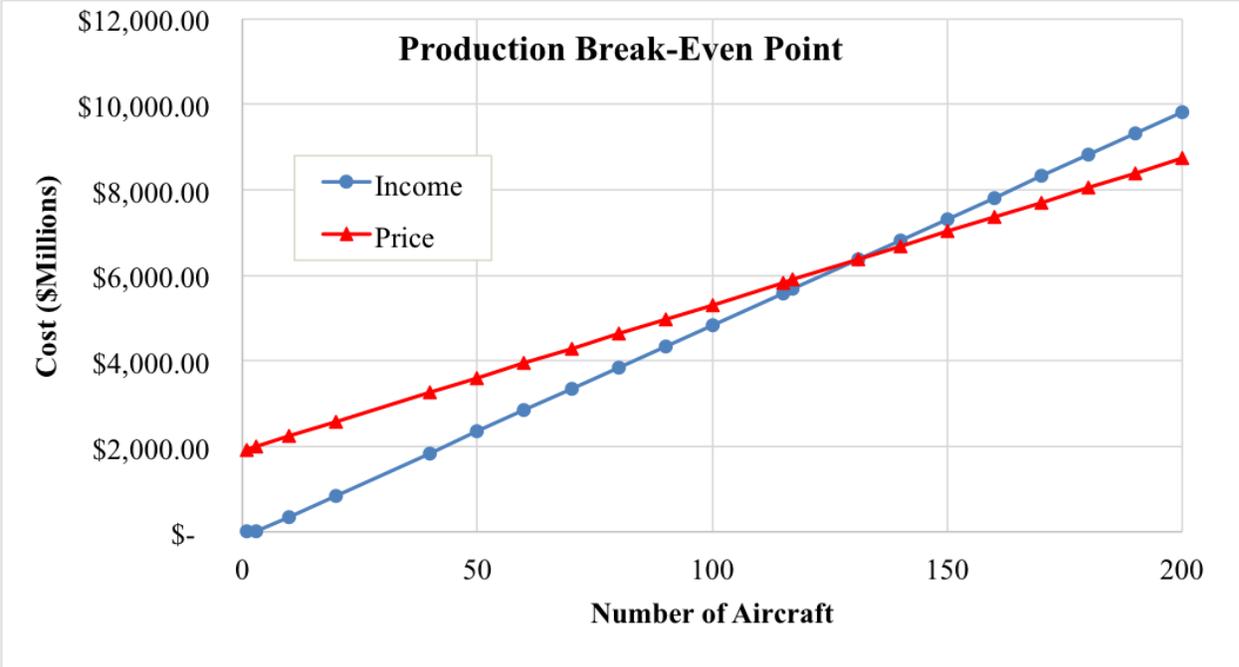
Figure 17.2-2: Production Break-Even Point Plot ($ million)

17.3 Flyaway Cost

The flyaway cost was approximated using Nicolai and Carichner's method by taking the quotient of the non-recurring costs and the total quantity of aircraft to be produced.[10] The flyaway cost for each unit was estimated to be $35.3 million in 2022 dollars. A detailed breakdown of the flyaway cost may be referenced in Figure 17.3-1.
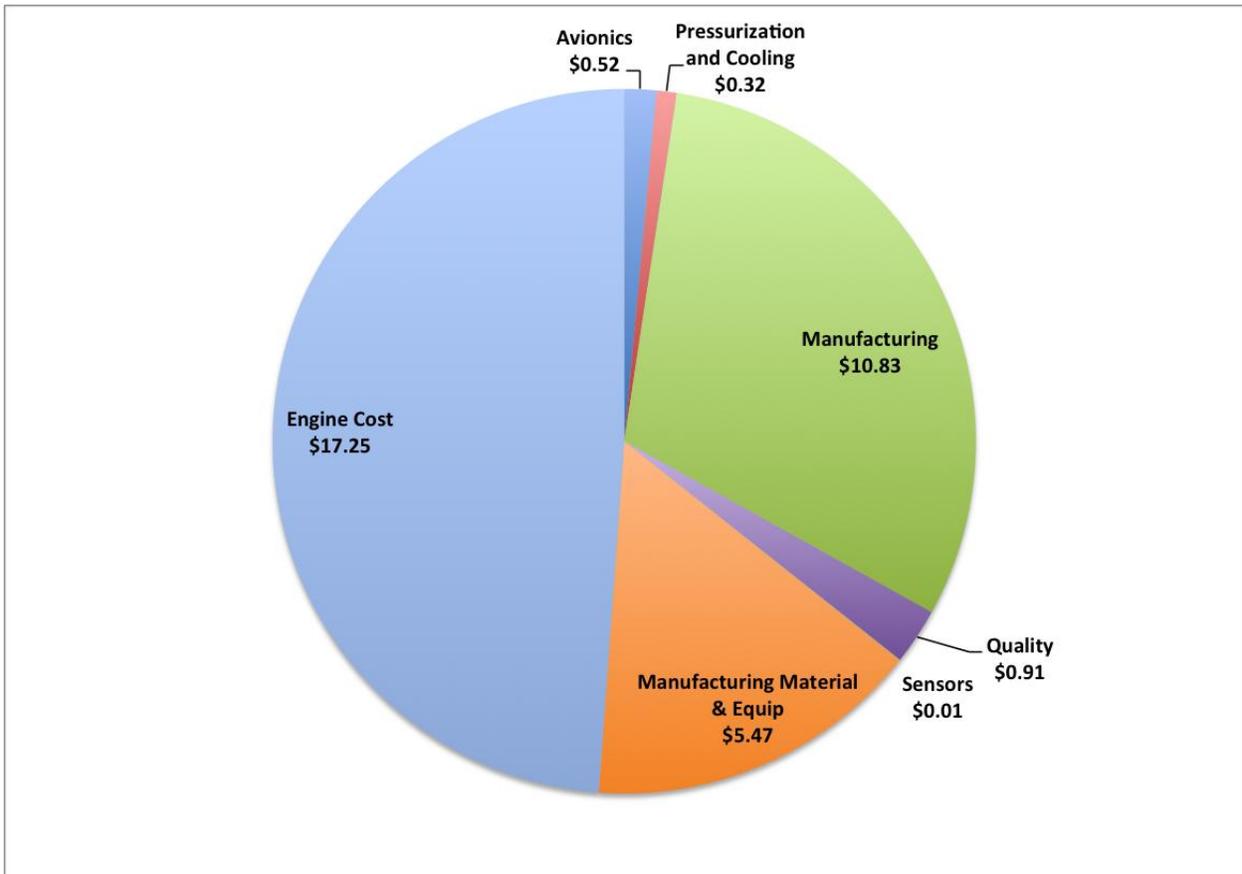
Figure 17.3-1: Flyaway Cost Breakdown ($ million)

The unit cost includes the RTD&E costs as well as the recurring costs such as

manufacturing and engine costs. The total unit cost for the FF-1 was analyzed to be $45.3 million

in 2022 dollars. With an implemented profit of 10%, the unit price was determined to be $49.8

million. Once again, selling 200 units yields a total profit of $1.08 billion. Figure 17.3-2 displays

the unit cost breakdown with the engine cost dominating the total cost.
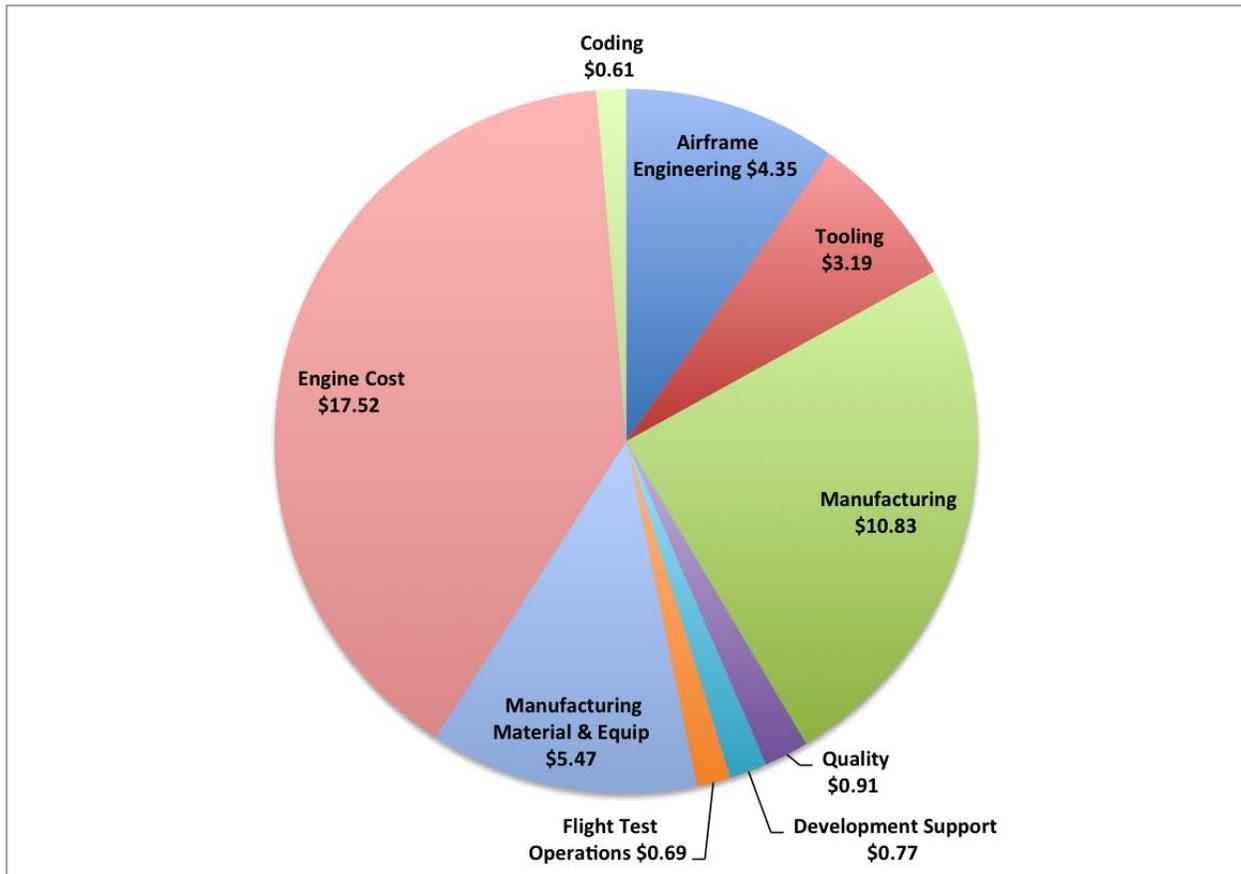
Figure 17.3-2: Unit Cost Breakdown ($ million)

A comparison of costs with a different engine configuration is displayed in Figure 17.3-3. To reiterate, the primary design will utilize the Rolls Royce Tay 620 while the back-up aircraft and engine combination will use the GE CF34-8C5B1.

Table 17.3-1: Unit Price Comparison

Aircraft And Engine Combination	Unit Price (2022 $ million)
FF-1 (Rolls Royce Tay)	49.8
FF-1 (GE CF34-8C5B1)	48.6

17.4 Direct Operating Cost (DOC)

Since our consumer basis will be a government entity, charges such as insurance, depreciation, landing fees, and retardant costs will not be included in the DOC. The direct operating cost was estimated to be $29.85k. Figure 17.4-1 has a breakdown of the DOC.
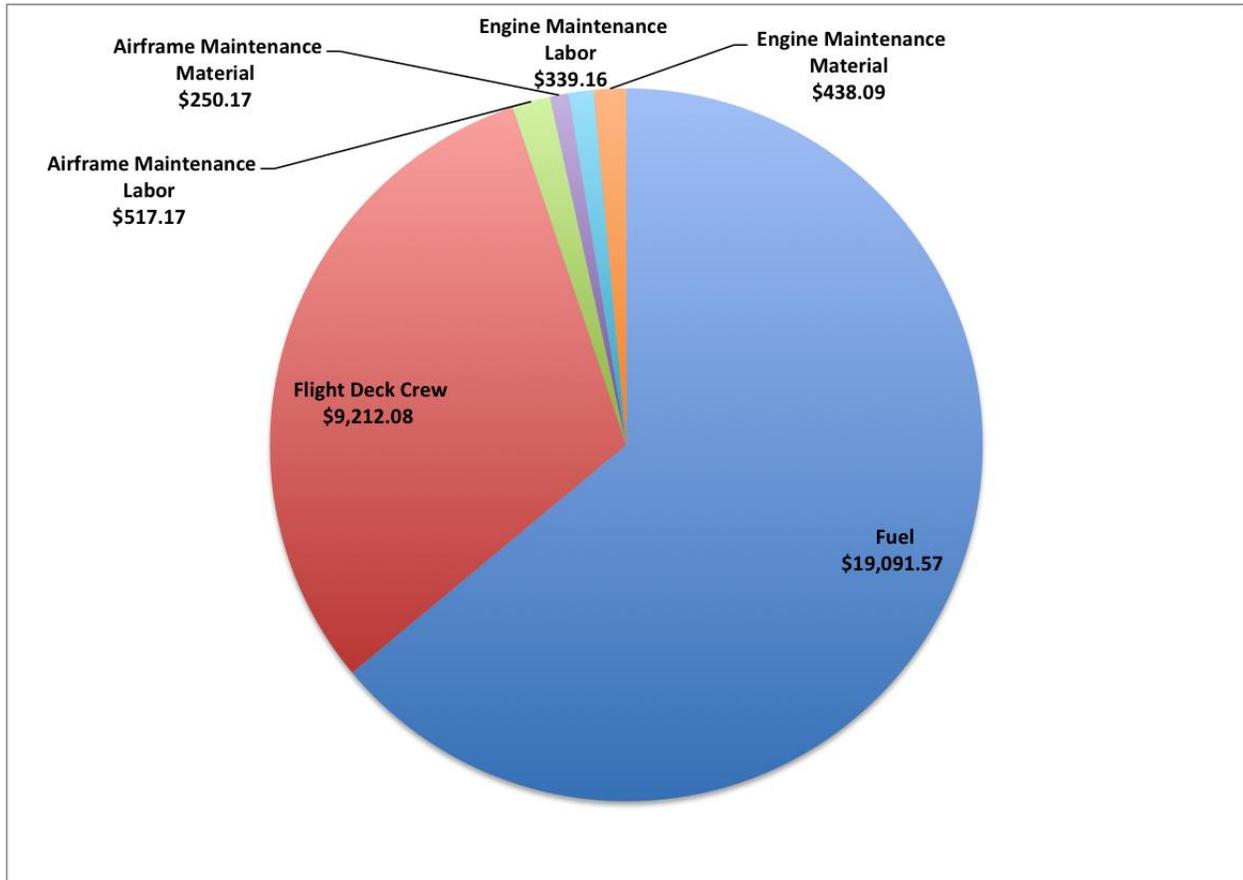
Figure 17.4-1: Direct Operating Cost Breakdown ($)

As mentioned before, the Rolls Royce Tay 620 gave a lower SFC than the GE CF34-8C5B1. Therefore, it gave the lowest possible operating cost per mission. Table 17.4-1 tabulates the DOC for each aircraft and engine combination as a comparison to justify the primary aircraft and engine configuration.

Table 17.4-1: Comparison of Primary and Secondary Aircraft and Engine Combinations

Aircraft And Engine Combination	Direct Operating Cost (2022 $)
FF-1 (Rolls Royce Tay)	29.85K
FF-1 (GE CF34-8C5B1)	41.02K

17.5 FF-1, Current Air Tankers, and Retrofitting Cost Comparison

The cost comparison between the FF-1 and the C-130 and DC 10 was obtained through the analysis of depreciation, the costs associated with retrofitting an existing aircraft into an air tanker, and the limited life of the aircraft in the year 2022. The cost of retrofitting an air tanker was approximated to be $23.71 million, not to mention the installation of a retardant delivery system which is another $6.38 million. The cost for the both the C-130 and DC-10 were obtained from *Military Aircraft* [5]. Table 17.5-1 exhibits the costs of the FF-1 configurations and the retrofitted competing aircraft.

Table 17.5-1: Acquisition Cost Of The FF-1 And Current Air Tankers

Aircraft	Acquisition Cost (2022 $ Million)
FF-1(Rolls Royce Tay 620)	49.8
FF-1(GE CF34-8C5B1)	48.6
C-130 (Retrofitted)	69.6
DC 10 (Retrofitted)	56

18. Compliance Matrix

Item	Requirement	Compliance (Yes, No)	Comments	Proposal Section
1	Performance Requirements			
1.1	Stall speed of 90 kt	Yes	89.98 kt	10.4
1.2	Dash speed >300kt	Yes	387 kt	10.4
1.3	Balanced field length of 5k ft	Yes	3,793 ft	10.2
1.4	Takeoff from 5k ft above mean sea-level with +35°F standard atmosphere	Yes	$\rho = 0.0094 \ \mu/ft^3$ for 5000 ft at +35ºF	2
1.5.1	Operational radius of 200 nm	Yes	200.25 nm	10.1
1.5.2	Ferry range of 2.5k nm	Yes	Maximum of 2615 nm	10.1
1.6.1	Payload of 5k gallons (water and retardant)	Yes	5k gallons of water and retardant	4.1
1.6.2	Retardant reload time ≤ 10 min	Yes	5.5 minutes	4.4
1.7	If piloted, 2 pilots	Yes	Piloted with 2 pilots	2
1.8	Turbine engine	Yes	Turbofan: Rolls Royce Tay 620	6.5
1.9	FAA certification for transport aircraft (Part 25)	Yes	Structural Analysis	11
2	Schedule Requirements			
2.1	Entry into service date 2022	Yes	2022	16
2.2	Lifetime ≥ 20 years	Yes	20 years (Maximum of 177,000 cycles)	11.3
3	Other Features and Considerations			
3.1	Off-the-shelf engine	Yes	Rolls Royce Tay 620	6.5
3.2	Special attention to fatigue	Yes	Fatigue Analysis	11.3
4	Primary Objectives			
4.1	Minimize time to establish a fire line	Yes	● Reduced reload time ● No refueling	4.4 10.1

			between sorties	
4.2	Minimize cost of ownership	Yes	Unit Price: $49.8 million DOC: $29.85K	16.5
5	Proposal and Design Data Requirements			
5.1	Description of the design mission	Yes	• 200 nm operational radius • 2,500 nm ferry range	2
5.2	Performance analysis and operational envelope	Yes	Max. Dash 387 knots	10-10.4
5.3	Weights and center of gravity travel	Yes	• **MTOW:** 89,197 lb • CG travels between 29.8% and 34.7	7 7.1
5.4	Structural characteristics including finite fatigue life cycles	Yes	Structural Analysis	11
5.5	Geometric description: control surfaces, internal arrangement	Yes	• Control Surfaces • Payload Integration	8.1-8.3 4
5.6	Aerodynamic characteristics	Yes	Aerodynamic Analysis	9
5.7	Propulsion system selection	Yes	• **Primary Engine:** Rolls Royce Tay 620 • **Backup Engine:** GE CF34-8C5B1	6.3-6.5
5.8	Stability and control	Yes	Stability and Control	8
5.9	Summary of cost estimate analysis	Yes	• **RDT&E Cost:** $1.89B • **Program Cost:** $8.9B	16

19. Conclusion

AeroTactic designed the FF-1 Rainbird in response to the 2015-2016 AIAA RFP for a large air tanker design. It meets the need for a large purpose built firefighting aircraft due to the recent and continuous increase of wildfires. The FF-1 strives to surpass all past, current, and proposed air tanker designs. As a result of being a purpose built air tanker, the FF-1is capable of carrying up to 47% more payload than the C-130 with a MTOW that is 73.8% less. The fuselage of the FF-1 has been designed to incorporate an integrated payload tank resulting in less excess space than retrofitted aircraft. Along with the gravity fed integrated tank, three reload ports on either side of the aircraft facilitated in reducing the FF-1 reload time. The five and a half minute reload time of the FF-1 is forty-three times faster than the C-130's pressurized MAFFS II system and two and a half minutes faster than the DC-10's gravity system's fastest recorded time of eight minutes, where it's typical reload time is 15-20 min.

The incorporation of winglets resulted in a five percent increase in the FF-1's L/D, increasing fuel efficiency and reducing weight. With higher fuel efficiency and lower MTOW, the FF-1 has unit price of $49.8M (in 2022 $) which is 28.5% less than retrofitting a C-130 ($69.6M in 2022 $) and 11.1% less than the DC-10 ($56M in 2022 $). In addition, the Rainbird costs 4.6% less than purchasing an already retrofitted C-130, $52.2 in 2022 $ (including d*epreciation of the C-130).*

References

[1] *Abbott, Ira H. A., and Albert Edward Von Doenhoff. Theory of Wing Sections; including a Summary of Airfoil Data. New York: McGraw-Hill, 1949. Print.*

[2] *Anderson, John D., Jr. "6.11 Time to Climb." Introduction to Flight. N.p.: n.p., n.d. 497-98. Print.*

[3] *Brandt, Steven A. Introduction to Aeronautics: A Design Perspective*. Reston, VA: American Institute of Aeronautics and Astronautics, 1997. Print.

[4] Bruhn, E. F. *Analysis and Design of Flight Vehicle Structures*. Philadelphia: G.W. Jacobs, 1973. Print.

[5] "C-130 Hercules." *Military Aircraft*. FAS Military Analysis Network, Feb. 2000. Web. 2016. <http://fas.org/man/dod-101/sys/ac/c-130.htm>.

[6] Dasgupta, Abhijit. *Effect of Tank Cross-Section and Longitudinal Baffles on Transient Liquid Slosh in Partly-Filled Road Tankers*. Thesis. Concordia University, 2011. Montreal, Quebec, Canada: n.p., n.d. Print.

[7] "FLIR Systems MD-324 Compact Thermal Night Vision Camera - Fixed Mounted, 320x240, White W/ Free S&H — 2 Models." *OpticsPlanet*. N.p., n.d. Web. 2016. <http://www.opticsplanet.com/flir-systems-md-324-compact-fixed-mounted-thermal-night-vision-camera-320x240-wh.html>.

[8] *Global Aviation Tires* (2015): n. pag. *Goodyear Aviation*. Apr. 2015.

Web. 2016. <https://www.goodyearaviation.com/resources/pdf/databook_4_2015.pdf>.

[9] "Lab 8 Notes-Basic Aircraft Design Rules." *Lab 8 Notes – Basic Aircraft Design Rules* (n.d.):

n. pag. *MIT OpenCourseWare*. MIT, 6 Apr. 2006. Web. 2016.

<http://ocw.mit.edu/courses/aeronautics-and-astronautics/16-01-unified-engineering-i-

*ii-i*ii-iv-fall-2005-spring-2006/systems-labs-06/spl8.pdf>.

[10] Lowey, H. "GE's CF34 Engine for Business and Regional Jets." *26th Joint Propulsion*

Conference (1990): n. pag. General Electric. Web.

[11] Nicolai, Leland M., (Leland Malcolm), Grant Carichner, and Leland M.

Nicolai.Fundamentals of Aircraft and Airship Design. Reston, VA: American Institute of

Aeronautics and Astronautics, 2010. Print.

[12] Raymer, Daniel P. *Aircraft Design: A Conceptual Approach*. Reston, VA: American

Institute

of Aeronautics and Astronautics, 1999. Print.

[13] Roux, Elodie. *Turbofan and Turbojet Engines: Database Handbook*. Paris: Ed. Elodie

Roux,   2007. Print.

[14] *Schaufele, Roger D. The Elements of Aircraft Preliminary Design. N.p.: n.p., n.d. Print.*

[15] Shigley, Joseph Edward., and Charles R. Mischke. *Mechanical Engineering Design*. New

York: McGraw-Hill, 1989. Print.

[16] *Statistical Summary of Commercial Jet Airplane Accidents Worldwide Operations*

   1959-2014. N.p.: n.p., n.d. *Boeing*. Aviation Safety, Aug. 2015. Web. 2016.

   "Tay"-*Rolls-Royce.* N.p,.n.d. Web.

[17] "*Water - Specific Volume and Weight Density." Water - Specific Volume and Weight*

Density.

   The Engineering ToolBox, n.d. Web. 2016.

[18] *Wood, Karl Dawson. Aircraft Design. Boulder, CO: Johnson, 1968. Print*.